# MODEL DEPENDENCE OF THE BINDING ENERGY OF NUCLEAR MATTER

Thesis for the Degree of Ph. D. MICHIGAN STATE UNIVERSITY MICHAEL DAVID MILLER 1969



#### This is to certify that the

#### thesis entitled

# MODEL DEPENDENCE OF THE BINDING ENERGY OF NUCLEAR MATTER presented by

Michael David Miller

has been accepted towards fulfillment of the requirements for

Ph. D. degree in Physics

Date September 16, 1969

**O**-169



#### **ABSTRACT**

## MODEL DEPENDENCE OF THE BINDING ENERGY OF NUCLEAR MATTER

By

#### Michael David Miller

It is possible to produce hard core, soft core, finite core, and momentum-dependent potentials which fit the two-nucleon elastic scattering data equally well and which are, therefore, indistinguishable from that standpoint. This thesis examines the feasibility of using nuclear matter calculations to distinguish between potentials which cannot be distinguished through two-nucleon elastic scattering experiments.

Using the method described by Brueckner and Masterson\*
for the static potentials and, with modifications, for the
momentum-dependent potentials, the mean binding energy per
nucleon in nuclear matter is calculated for each of the S,
P, and D states using several phenomenological two-nucleon
potentials which have identical on-energy-shell matrix
elements. The binding energy is found to be very sensitive
to the form of the short range repulsion in the potential.
Replacing a hard core potential by a short range momentumdependent one having identical on-energy-shell matrix elements
is found to increase the contribution of the S and P states
to the binding energy of nuclear matter. There was little
change in the contribution of the D states. With the proper

form for the momentum dependence, increases in the binding energy of over 12 MeV per particle were obtainable.

The hard core Hamada-Johnston potential predicts a binding energy of 8.5 MeV per particle for a Fermi momentum of 1.4 F<sup>-1</sup>. This is fairly typical of hard core potentials which fit the two-nucleon elastic scattering data fairly well, but is in poor agreement with the empirical value of 16 MeV per nucleon. Replacing the S state potential alone by an equivalent momentum-dependent one results in a calculated value for the binding energy which is in excellent agreement with the empirical value.

K. A. Brueckner and K. S. Masterson, Jr., Phys. Rev. <u>128</u>, 2267, (1962).

# MODEL DEPENDENCE OF THE BINDING ENERGY OF NUCLEAR MATTER

By

Michael David Miller

#### A THESIS

Submitted to
Michigan State University
in partial fulfillment of the requirements
for the degree of

DOCTOR OF PHILOSOPHY

Department of Physics

4-27-70

#### ACKNOWLEDGMENTS

I would like to thank Professor Peter S. Signell for his help in selecting and solving this problem.

For her help in the preparation of the manuscript, I would like to thank my wife who, along with my children, Matthew and Marna, also provided greatly appreciated companionship.

#### TABLE OF CONTENTS

LIST	OF T	ABLES	iv
LIST	OF F	IGURES	v
I.	INT	RODUCTION	1
II.	THE	ORY	9
	A.	Properties of Nuclear Matter	9
	В.	Summary of Brueckner-Goldstone Theory	11
	c.	Baker Transform	22
III.	POT	ENTIALS	30
IV.	CAL	CULATIONS	39
	A.	Static Potential Calculations	39
	В.	Momentum-Dependent Potential Calculations	44
	c.	Phase Shift Calculations	50
v.	RES	ULTS	51
APPEN	DIX	•••••	68
REFE	RENCE	s	74

#### LIST OF TABLES

Table		Page
ı.	$\chi^{\mathbf{z}}$ for various phenomenological two-nucleon potentials	4
II.	Hamada-Johnston potential parameters	38
III.	Mean binding energy per nucleon predicted by the S <sub>0</sub> potentials	53
IV.	Percent increase of the <sup>1</sup> S <sub>0</sub> K matrix elements over the values obtained with the 0.4 F hard core potential	55
v.	Mean binding energy per nucleon predicted by momentum-dependent potentials generated from the Hamada-Johnston potential	56

#### LIST OF FIGURES

Figure		Page		
1.	1S <sub>0</sub> phase shifts predicted by the static potentials and the values deduced from two-nucleon scattering experiments			
2.	Static <sup>1</sup> S <sub>0</sub> potentials	31		
3.	Momentum-dependent <sup>1</sup> S <sub>0</sub> potentials	34		
4.	Momentum-dependent <sup>1</sup> D <sub>2</sub> potentials	59		
5.	Momentum-dependent <sup>3</sup> D <sub>1</sub> potentials	60		
6.	Momentum-dependent <sup>3</sup> D <sub>2</sub> potentials	61		
7.	<sup>1</sup> P <sub>1</sub> phase shift vs. energy	63		
8.	<sup>3</sup> P <sub>0</sub> phase shift vs. energy	64		
9.	<sup>3</sup> P <sub>1</sub> phase shift vs. energy	65		
10.	<sup>3</sup> P <sub>2</sub> phase shift vs. energy	66		

#### SECTION I

#### INTRODUCTION

Ever since the discovery that the atomic nucleus was composed of neutrons and protons, there have been attempts to explain the properties of nuclei in terms of the interaction of these particles. Although it is now clear that an accurate theory of the nucleus will involve more than the nonrelativistic Schroedinger equation for neutrons and protons interacting through a two-nucleon potential, this is at least a good starting point. Even if the two body forces prove to be unable to account for all of the nuclear data, their failure should at least provide some clue as to the nature of the many body forces.

The two-nucleon potential need only be valid up to about 350 MeV in the laboratory frame. Above this energy pion production becomes significant and the use of the non-relativistic Schroedinger equation is probably not justified. However, since the top of the Fermi sea in nuclear matter corresponds to an energy of only about 160 MeV, the 350 MeV upper limit on the theory should not be too restrictive.

It is generally agreed that if a two-nucleon potential is to fit the two-nucleon elastic scattering data, it must assume the form of the one-pion-exchange potential at large

distances. At small distances it must have some form of short range repulsion, at least in the S and  $^3P_0$  states. Within this broad framework there have been many attempts to produce a purely phenomenological two-nucleon potential which not only fit the two-nucleon elastic scattering data, but also produced reasonably good results in nuclear calculations.

The phenomenological potentials are best classified according to the form used for the short range repulsion. The most common types have been the infinitely repulsive hard core, the finite core, the soft core, and the momentum-dependent repulsion. The ability of these potentials to describe the two-nucleon interaction has differed widely. The best way of comparing the quality of one phenomenological potential with another is to compare the goodness-of-fit parameter,  $\chi^2$ , obtained when each of the potentials is used to predict the same set of experimental data. For N data,

$$\chi^2 = \sum_{n=1}^{N} \left( \frac{P_n - E_n}{\epsilon_n} \right)^2$$

where  $\epsilon_n$  is the experimental standard deviation associated with the experimental datum  $\mathcal{E}_n$ , and  $\mathcal{P}_n$  is the value predicted by the potential. The closer the predicted values are to the experimental values, the smaller  $\chi^2$  will be. The more accurate data with their lower uncertainties will be more sensitive to variations in the potential parameters than the less accurate data.

Table I shows some of the more popular potentials and their associated  $\mathcal{L}^2$  values for the current set of statistically valid two-nucleon elastic scattering data below 350 MeV. The Bressel-Kerman finite core potential seems to be the one preferred by the elastic scattering data. However, the hard core Hamada-Johnston potential is five years older and is still almost as good a fit to the data. Probably only some small changes in the values of the potential parameters in order to account for the additional, more accurate data would result in very close agreement between these two potentials. In fact, previous work with the very accurate data available at 210 MeV has shown that at that energy the majority of the difference in the two potentials could be eliminated by changes in the  $^3P_2$  state alone. Presumably, similar results would be found at other energies.

Thus, at the present time, the two-nucleon elastic scattering data does not appear to be able to distinguish between properly parameterized hard core and finite core potentials. This was emphasized for the  $^1S_0$  state when a family of hard, soft, and finite core potentials was generated, each of which gave a precise fit to the  $^1S_0$  phase shifts deduced from the elastic scattering data below 330 MeV. The same thing could probably be done for the other states. Furthermore, Baker has shown that given any hard core potential, a family of momentum-dependent potentials can be generated which will produce elastic scattering phase shifts which are identical at all energies to those

Table I.  $\chi^2$  for various phenomenological two-nucleon potentials.

Potential	Туре	χ <sup>*</sup> for 648 pp data	え <sup>*</sup> for 952 np data
Bressel-Kerman <sup>a</sup>	finite core	1382	2031
Hamada-Johnston <sup>b</sup>	hard core	1929	2149
Bethe-Reid <sup>C</sup>	hard core	1763	4249
Yale <sup>d</sup>	hard core	2471	2511

a Reference 2.

b Reference 3.

<sup>&</sup>lt;sup>C</sup> R. V. Reid, quoted in Bhargava and Sprung, Reference 2.

d K. E. Lassila, M. H. Hull, Jr., H. M. Ruppel, F. A. MacDonald, and G. Breit, Phys. Rev. 126, 881 (1962).

produced by the original hard core potential.6

It has been suggested that the many-body problem might be helpful in distinguishing between potentials that are identical from the standpoint of two-nucleon elastic scattering. The advantage of the many-body problem is that it allows for scattering off the energy shell. This is scattering in which the two-body interaction occurs between two particles in excited states at an energy different from that of the initial and final states.

There have been previous attempts to use nuclear matter calculations to distinguish between hard core and momentum-dependent potentials. 8 Although the results indicated a desirable increase in binding for the momentumdependent potentials, they were not conclusive qualitatively. For one thing, the potentials used did not have identical on-energy-shell matrix elements, although it is clear from Baker's work that it is possible to develop potentials of these two forms that do. Thus one was left to wonder whether the nuclear matter calculations merely emphasized the on-energy-shell differences in the potentials, which could be distinguished through sufficiently accurate elastic scattering experiments, or if the differences in the nuclear matter calculations were really due to off-energy-shell processes, which are not involved in two-body scattering. To further complicate matters, the momentum-dependent potential calculations were carried out using perturbation theory while the hard core potentials were treated using

Brueckner's method. The different approximations made in the two methods alone could easily result in discrepancies of over 2 MeV per nucleon in the average binding energy, which is more than the difference between some models when a consistent procedure is used.

Both of these sources of uncertainty have been avoided In the treatment of the <sup>1</sup>S<sub>0</sub> state alone, the momentum-dependent potentials were derived from the 0.4 F hard core 150 potential of Reference 5 using Baker's transformation. As shown in Figure 1, the  $^{1}S_{0}$  phase shifts below 330 MeV obtained from the soft core and finite core potentials agree with those obtained from the 0.4 F hard core potential to within a small fraction of the standard deviation obtained from the experimental data. Above 330 MeV they begin to diverge slowly. Of course, the 150 phase shifts obtained from the momentum-dependent potentials are identical to those produced by the 0.4 F hard core potential at all energies. So for use in nuclear matter calculations these potentials can be considered to have identical onenergy-shell matrix elements. In working with the other states, the momentum-dependent potentials were obtained from and compared with the Hamada-Johnston hard core potential alone.

In calculating the binding energy for nuclear matter, the method described by Brueckner and Masterson<sup>9</sup> was used for all of the potentials. The modifications made in treating the momentum-dependent potentials involved no

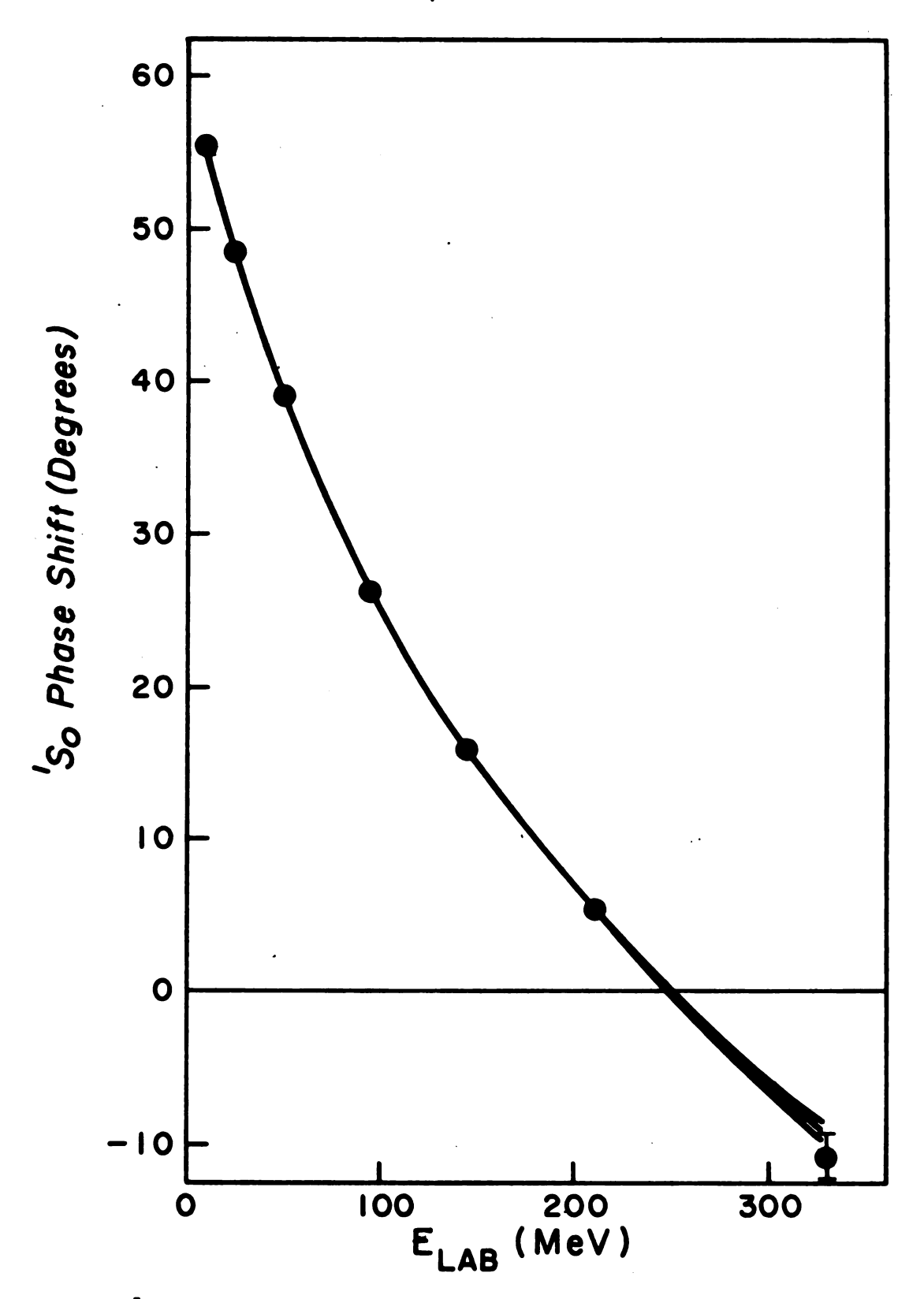


Figure 1. <sup>1</sup>S<sub>0</sub> phase shifts predicted by the static potentials and the values deduced from two-nucleon scattering experiments. See Reference 5.

additional approximations above those involved in the calculations using the other potential forms. Thus the results obtained here should be an accurate quantitative description of the ability of nuclear matter to distinguish between potentials that cannot be distinguished through two-nucleon elastic scattering experiments.

#### SECTION II

#### THEORY

#### A. Properties of Nuclear Matter

Nuclear matter is a hypothetical system of  $\frac{A}{2}$  neutrons and  $\frac{A}{2}$  protons where A is allowed to become infinitely large. If the coulomb repulsion of the protons is ignored, it is thought that in its lowest energy state a stable configuration would result, characterized by a uniform density, A, and a mean binding energy per particle,  $\omega$  . Because nuclear matter is assumed to be homogeneous and isotropic, the single particle wave functions of nuclear matter are just plane Thought of as a first approximation to a heavy nucleus, nuclear matter provides a medium in which the ability of a two-nucleon potential to predict some of the properties of a nucleus can be tested without all of the difficulties inherent in the calculation of the properties of a finite nucleus. A potential which fails to satisfactorily predict the binding energy and density of nuclear matter need not be dragged through a finite nucleus calculation.

The average binding energy per particle that nuclear matter would be expected to have if it really existed is deduced from the semi-empirical mass formula. According to this formula, the binding energy of a nucleus is

$$\mathcal{E} = a_1 A + a_2 A^{\frac{2}{3}} + a_3 (\frac{A}{3} - Z)^2 A^{-1} + a_4 Z^2 A^{-\frac{1}{3}} + a_5 A^{-\frac{3}{3}}$$
 (II-1)

The first term is the volume energy term, the second a correction to account for surface tension, the third is the symmetry energy. The fourth term represents the contribution of the coulomb repulsion between protons, and the last term is a small correction which accounts for pairing effects. With properly chosen constants, this equation predicts the binding energies of nuclei with a standard deviation of 2.61 MeV per nucleon. However, the deviations from the mean values have systematic trends which are evidence of shell structure and no attempt was made to account for this property of nuclei in equation (II-1).

For nuclear matter, the number of nucleons, A, is infinitely large, so the surface and pairing effects are negligible. As stated before, coulomb effects are ignored, and equal numbers of neutrons and protons are assumed. The result of these assumptions is that the expected binding energy of nuclear matter is just the volume energy term of the semi-empirical mass formula. This quantity has been determined to be about -16 MeV per nucleon. 11, 12 The corresponding energy for finite nuclei is about -8 MeV per particle. 13 The difference is due solely to the inclusion of coulomb, surface, symmetry, and pairing effects in finite nuclei.

In addition to the binding energy of nuclear matter, the saturation density must also be calculated. The latter

energy as a function of particle density. The minimum of the curve determines the saturation density and the associated binding energy. These can then be compared with the empirically determined quantities. Starting from the density of the interior of a heavy nucleus and taking into account the effects of coulomb repulsion and surface tension, the saturation density of nuclear matter has been determined to be about 0.170 F<sup>-3</sup>. <sup>14</sup> Because nuclear matter is treated as the ground state of a Fermi gas which is perturbed by two-body interactions between the nucleons, a more convenient quantity to use in describing the density of nuclear matter is the Fermi momentum, k, which is related to the saturation density, A, by

$$k_{F} = \left(\frac{3\pi^{2}}{2}\right)^{\frac{1}{2}} = 1.36 F^{-1}$$

### B. Summary of Brueckner-Goldstone Theory 15

The theory of nuclear matter begins with A nucleons composing a Fermi gas in its ground state, which is assumed to be non-degenerate. The density of the Fermi gas is  $\rho = \frac{A}{\Omega}$ , where  $\Omega$  is the volume of a very large box in which all the nucleons are contained. If the particles do not interact, then the energy of the distribution is just the sum of the kinetic energies of the particles

$$E_{\mu} = \sum_{i=1}^{A} T(k_i) = \sum_{i=1}^{A} \frac{h^{i} k_i^{i}}{2M}$$

To obtain the ground state of nuclear matter, a two-nucleon potential,  $\nu_{ij}$ , acting between states i and j is introduced. The total Hamiltonian then becomes

$$\mathcal{H} = \sum_{i=1}^{A} T(k_i) + \sum_{i = j} \sum_{j=1}^{A} \nu_{ij}$$

which can be written

$$H = H_0 + H_1$$
 (II-2)

where

$$H_0 = \sum_{i=1}^{A} T(k_i) + \sum_{i=1}^{A} V(k_i)$$

$$H_{i} = \sum_{i \neq j} \sum_{i=1}^{A} \nu_{ij} - \sum_{i=1}^{A} V(\lambda_{i})$$

The quantity  $V(k_i)$  is the single particle potential acting on particle i and is dependent only on the momentum of the particle on which it acts. It is introduced only in order to simplify the calculation by improving the convergence of the series expansion and will have no effect on the energy of the distribution. The actual form of the single particle potential will be discussed later.

If  $I\!\!\!/$  is the perturbed ground state wave function, then the energy per particle,  $I\!\!\!/$ , is found by solving

$$H\bar{\mathbf{Y}} = \mathbf{E}\mathbf{\hat{Y}} \tag{II-3}$$

For the unperturbed ground state this reduces to

where  $\not Q$  is a Slater determinant of the single particle states,  $\not q$  . The normalizations of  $\not L$  and  $\not Q$  are chosen

such that

$$\langle \phi_0 / \phi_0 \rangle = 1$$

and

Then from equations (II-2) and (II-3)

giving

Equation (II-3) can be rewritten

$$(\mathcal{E} - \mathcal{H}_0)/\hat{\mathcal{I}} > = \mathcal{H}_1/\hat{\mathcal{I}} > \tag{II-4}$$

Adding the homogeneous equation  $(E_{\bullet} - H_{\bullet})/f_{\bullet} > = 0$  to the right hand side of equation (II-4), one obtains

$$|\bar{\Psi}\rangle = \frac{E_{\circ} - H_{\circ}}{E - H_{\circ}} |\bar{\mathcal{P}}_{\circ}\rangle + \frac{1}{E - H_{\circ}} H_{\circ} |\bar{\Psi}\rangle$$

$$= |\bar{\mathcal{P}}_{\circ}\rangle - \frac{E - E_{\circ}}{E - H_{\circ}} |\bar{\mathcal{P}}_{\circ}\rangle + \frac{1}{E - H_{\circ}} H_{\circ} |\bar{\Psi}\rangle$$

Then using equation (II-4),

$$\begin{split} /\bar{\Psi}\rangle &= /\bar{\Phi}_{o}\rangle - \frac{1}{\bar{\epsilon} - H_{o}}/\bar{\Phi}_{o}\rangle \langle \bar{\Phi}_{o}/H_{c}/\bar{\Psi}\rangle + \frac{1}{\bar{\epsilon} - H_{o}}H_{c}/\bar{\Psi}\rangle \\ &= /\bar{\Phi}_{o}\rangle + \frac{P}{\bar{\epsilon} - H_{o}}H_{c}/\bar{\Psi}\rangle \end{split} \tag{II-5}$$

where  $P_{\Xi}/-/\Phi_{\bullet}/\langle \Phi_{\bullet}/\rangle$  is an operator which prevents the unperturbed ground state from occuring as an intermediate state. Using equation (II-5) in equation (II-4) and

multiplying on the left by  $\langle \phi_{\!\scriptscriptstyle o} /$  , the energy shift is found to be

which can be expanded as a perturbation series in  $\mathcal{H}_i$ , giving

$$\mathcal{E}^{-}\mathcal{E}_{o} = \langle \phi_{o}/H_{i}/\overline{\phi_{o}} \rangle + \langle \overline{\phi_{o}}/H_{i}\frac{P}{\mathcal{E}^{-}H_{b}}H_{i}/\overline{\phi_{o}} \rangle + \cdots$$
 (II-6) to second order.

At this point it becomes more convenient to let the subscripts refer to states rather than particles. Subscripts a through j refer to states above the Fermi sea, k through n to states in the Fermi sea. The rest refer to any state. Sums over these subscripts imply sums over the entire range of states covered by the subscripts. Since each momentum state below the Fermi momentum will contain two neutrons and two protons (one of each spin), there will be four distinct states of each momentum up to the top of the Fermi sea for a total of A filled states. A particle will have a momentum greater than  $k_{\epsilon}$  only if it has been excited, leaving a hole in the state it originally occupied below the Fermi sea. Equation (II-6) can be rewritten as an expansion in terms of the single particle potential, V, and the two-body potential,  $\nu_{pq}$ . Then in the notation of second quantization (see Appendix) equation (II-6) becomes to first order

$$E-E_0=\frac{1}{2}\sum_{m,n}\langle mn|\nu|mn\rangle-\frac{1}{2}\sum_{m,n}\langle mn|\nu|nm\rangle-\sum_{n}\langle n|V|n\rangle +\cdots$$
(II-7)

The factor  $\frac{1}{2}$  is needed because the summation is carried out over all states with the result that each distinct matrix element is counted twice.

A problem immediately arises because of the strong short range repulsion of many two-nucleon potentials. Matrix elements of these potentials will be extremely large and equation (II-7) will not converge even though the energy shift,  $\mathcal{E} - \mathcal{E}_{\bullet}$ , may be small. Brueckner's solution to this problem was to replace the expansion in terms of the two-nucleon potential by an expansion in terms of the reaction matrix defined by

$$K(W) = \nu_{pq} - \nu_{pq} \left(\frac{Q}{e}\right) K(W)$$
 (II-8)

where Q is the Pauli operator with the properties

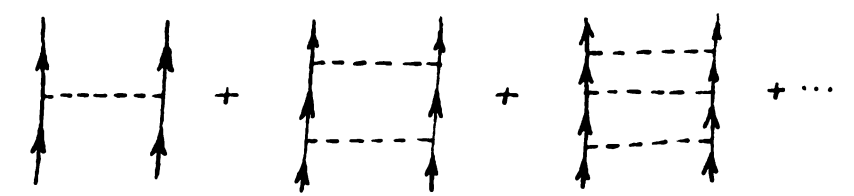
and

where W is the starting energy. The energy denominator is determined by calculating the sum of the particle energies minus the sum of the hole energies. The starting energy is obtained by subtracting  $\mathcal{E}_{\rho} + \mathcal{E}_{\varphi}$  from the result.

Introducing the reaction matrix is equivalent to regrouping the matrix elements of the two-nucleon potential between particles in the original expansion in such a way that each term in the new series makes a small enough contribution to the total energy that the series quickly

converges. Interactions between holes are not included in this partial summation because their momenta are restricted to  $k \le k_F$  whereas the momentum of a particle can be many times that. Hence the phase space available to the holes is much more limited than that available to the particles with the result that interactions between particles are expected to be the major contributors to the energy shift.

The grouping of terms is probably more easily explained in terms of diagrams. Any series of interactions between particles of the form



is replaced by one diagram containing the interaction represented by



The dashed line represents the two nucleon potential and the wavy line the reaction matrix. The diagrams to first order in the reaction matrix and single particle potential are



The contribution of the first order diagram in the single particle potential cancels the corresponding term arising from  $\mathcal{H}_{o}$  regardless of the form of the single particle potential. The second of the first order diagrams

represents the sum of diagrams involving the two-nucleon potential

$$\bigcap_{m} \bigcap_{n} = \bigcap_{m} \bigcap_{n} + \bigcap_{m} \bigcap_{n} \bigcap_{m} \bigcap_{m} \bigcap_{n} \bigcap_{m} \bigcap_{m} \bigcap_{n} \bigcap_{m} \bigcap_{m}$$

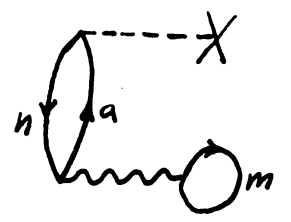
The third is just the exchange diagram

All second order diagrams of the reaction matrix are either redundant or do not conserve momentum, so they do not contribute to the energy of nuclear matter. For example, the diagram

is clearly included in the first order diagram



An example of a second order diagram that does not conserve momentum is



Since the state  $\alpha$  is above the Fermi sea and state n is in it, momentum conservation is clearly violated between the two interactions.

It is possible to choose the single particle potential in such a way that most of the important three-body diagrams If this is done the contribution of these and will cancel. higher order diagrams to the energy of nuclear matter is expected to be only about 1 MeV per particle. 16 Even if some other form is chosen for the single particle potential, the contribution to the energy which is not included in the first order diagrams is not expected to exceed 4 MeV. 16, 17 This is only about 10% of the total potential energy, and if it is not considerably more model dependent than the contribution of the first order diagrams it will not alter the conclusions drawn on the basis of the first order diagrams Because only first order diagrams were considered here, the single particle potential was chosen in such a manner that the contribution of the two reaction matrix diagrams were cancelled by the diagram involving the single particle potential. That is

$$\langle n/V/n \rangle = \sum_{m} \langle mn/k/mn \rangle - \sum_{m} \langle mn/k/nm \rangle$$

Thus the energy shift will be just the sum of the matrix elements of the unperturbed Hamiltonian,  $\mathcal{H}_0$ , between all single particle states in the Fermi sea. This is just the sum of the kinetic energies and single particle potential energies of each particle in its lowest state.

In order to calculate the reaction matrix elements, it is convenient to define a correlated two-body wave function,

The unperturbed two-body wave function is just the product of two unperturbed single particle wave functions.

As stated before, the unperturbed single particle wave functions are just plane waves. If the nuclear matter under consideration is assumed to be enclosed in a large box of volume 1, then the single particle wave functions are

$$\phi_{\beta}(\vec{r}_i) = \frac{1}{\sqrt{\Delta}} e^{i\vec{k}_{\beta} \cdot \vec{r}_i}$$

so the two-body unperturbed wave functions are

This can be rewritten

$$\mathcal{Q}_{pp}(\vec{r},\vec{r}_{i}) = \frac{1}{\pi} e^{i\vec{k}\cdot\vec{p}} e^{i\vec{k}\cdot\vec{r}}$$
(II-9)

where

$$\vec{R} = \frac{1}{2} (\vec{r}_1 + \vec{r}_2) \qquad \vec{r} = \vec{r}_1 - \vec{r}_2$$

$$\vec{K}_{pp} = \vec{k}_p + \vec{k}_p \qquad \vec{k} = \frac{1}{2} (\vec{k}_p - \vec{k}_p) \qquad (III-10)$$

These new quantities are the center of mass coordinate of the two particles,  $\vec{R}$ , and the total momentum  $\vec{K}_{pp}$ . The other two quantities are the relative position and momentum. Equation (II-9) can be rewritten

$$\oint_{P_{p}}(\vec{r},\vec{r}) = \frac{1}{52}e^{i\vec{K}_{P_{p}}\cdot\vec{R}}\oint_{P_{p}}(\vec{r},\vec{k})$$
(II-11)

This defines  $(\vec{r}, \vec{k})$  as that part of the unperturbed two-body wave function which is a function only of the relative position and momentum of the two particles. The two-body correlated wave function is then defined

$$I_{pq} = \bar{p}_{pq} - \frac{Q}{e} K \bar{p}_{pq}$$

$$= (1 - \frac{Q}{e} K) \bar{p}_{pq}$$
(II-12)

Multiplying both sides by the two-nucleon potential and using the definition of the reaction matrix, equation (II-8), results in

So equation (II-12) can be rewritten

$$I_{pp} = I_{pp} - \frac{Q}{e} \nu I_{pp} \qquad (II-13)$$

Because the operators v, e, and Q all conserve total momentum, the dependence of  $I_{pp}$  and  $I_{pp}$  on r and R will be the same. The correlated wave function can then be written

$$Y_{pq} = \frac{1}{\pi} e^{i\vec{k}pq \cdot \vec{R}} Y_{pq}$$
 (II-14)

where  $V_{p_p}$  is a function of the relative position vector and momentum only.

Using equations (II-11) and (II-14) in equation (II-13), one finds, as expected, that the reaction matrix elements are independent of s and  $\vec{R}$ .

$$\langle rs/K/p_{q} \rangle = \int g_{s}(\vec{r}) \nu(r,k) \psi_{p_{q}}(\vec{r}) J^{s}\vec{r}$$
 (II-15)

where

$$\psi_{p}(\vec{r}) = \psi_{p}(\vec{r}) - \int G_{pp}(\vec{r}, \vec{r}') \, \nu(r; k) \, \psi_{pp}(\vec{r}') \, d^{p}\vec{r}' \qquad (II-16)$$

and

$$G_{pp}(\vec{r},\vec{r}') = \frac{1}{2\pi^3} \int d^3k \, \frac{Q(\vec{k},\vec{K}_{pp})}{e(\vec{k},\vec{K}_{pp})} e^{i\vec{k}\cdot(\vec{r}-\vec{r}')}$$
(II-17)

As stated previously, the total momentum,  $\vec{k}_{ff}$ , is conserved in the two-nucleon interaction; however, the relative momentum,  $\vec{k}$ , can change to some new value,  $\vec{k}'$ . The Pauli operator,  $\mathcal{Q}$ , eliminates from the integrand all transitions to occupied states in the Fermi sea. If  $\vec{k}_i$  and  $\vec{k}_i$  are the momenta of particles 1 and 2 in some intermediate state, then

$$Q=0$$
 if  $k_1 < k_F$  or  $k_2 < k_F$   
 $Q=1$  if  $k_1 > k_F$  and  $k_2 > k_F$ 

where, by equation (II-10),

$$\vec{k}_{1} = \pm \vec{K}_{12} + \vec{k}$$
 $\vec{k}_{2} = \pm \vec{K}_{12} - \vec{k}$ 

The energy denominator, e, is dependent not only on the kinetic energy of the states involved, but also on the single particle potentials associated with them. However,

the single particle potentials are functions of momentum which are determined by the reaction matrix elements. one must assume some initial value for the single particle potentials and calculate the reaction matrix. New single particle potentials can be calculated from the reaction matrix, and these are then used in recalculating the energy denominator. This procedure is repeated until the single particle potentials generated by the reaction matrix agree with those used to calculate that reaction matrix. If it were not for the complicated dependence of the operators Q and c on the total and relative momenta, nuclear matter calculations would be greatly simplified. In fact, if one sets Q: | and defines the energy denominator to be just the kinetic energy of the particles involved, as is the case for the free two-nucleon interaction, one finds that  $G_{pp}(\vec{r}, \vec{r}')$ can be calculated analytically and equation (II-16) becomes

where  $\vec{k}$  is the relative momentum of the two nucleons before scattering. This is the integral equation for two-particle scattering.

#### C. Baker Transform

The Schroedinger equation for two nucleons interacting through a momentum-dependent potential can be shown to have solutions which are identical at large distances to those produced by the Schroedinger equation for two nucleons interacting through a static potential outside a hard core.

The Schroedinger equation for the momentum dependent potential can be written

$$\left\{ \frac{1}{4m} \left[ \mu(r) \, \rho^2 + 2 \vec{\rho} \cdot \mu(r) \, \vec{\rho} + \rho^2 \mu(r) \right] + V_*(r) \right\} \, \mathcal{V}(\vec{r}) = E \, \mathcal{V}(\vec{r})$$
 (II-18)

where  $\mu \geqslant l$  for a repulsive force and  $\mu(\omega) = 0$ . M is the nucleon mass, and  $\sqrt[3]{r}$  is a static potential. The form of the term involving the momentum operator is required for hermiticity and time reversal invariance. If  $\mu(r) \equiv l$  for all values of r, then equation (II-18) just reduces to the Schroedinger equation for a static potential. Using  $\rho = i\hbar \nabla$ , equation (II-18) can be written

$$\mu(r) \nabla^{2} Y(\vec{r}) + \nabla \mu(r) \cdot \nabla Y(\vec{r}) + \frac{1}{7} Y(\vec{r}) \nabla^{2} \mu(r) + \frac{M}{4^{2}} \left[ \vec{c} - V_{s}^{8}(r) \right] Y(\vec{r}) = 0$$
(II-19)

Since and  $V_s^{st}$  are functions of ronly, equation (II-19) may be separated into radial and angular components. Writing the equation for a particular partial wave and noting that the angular component is identical to the one obtained in the static problem, the radial equation becomes

$$\frac{d^{2}}{dr^{2}}\frac{1}{2}(r) + \left(\frac{\mu'(r)}{\mu(r)} + \frac{1}{r}\right)\frac{d}{dr}\frac{\psi'(r)}{2r\mu(r)} + \frac{M}{\mu(r)}\frac{\left[E - V_{s}^{B}(r)\right] - \frac{\mu(x+r)}{r^{2}}\left[\psi'(r) = 0\right]}{\left[E - V_{s}^{B}(r)\right] - \frac{\mu(x+r)}{r^{2}}\left[\psi'(r) = 0\right]}$$
(II-20)

where

Now make the transformation

So

where

Then equation (II-20) becomes

$$\frac{\mu(r) \, \xi(\rho)}{\left[r'(\rho)\right]^{2}} \, \frac{J^{2} U_{2}(\rho)}{J^{2} \rho^{2}} \, - \, \frac{\mathcal{L}(\mathcal{L}+1) \, \mu(r)}{\left[r'(\rho)\right]^{2}} \, \xi(\rho) \, U_{2}(\rho)$$

$$+ \left[\frac{2 \, \xi'(\rho) \, \mu(r)}{\left[r'(\rho)\right]^{2}} + \left(\frac{2 \, \mu(r)}{r(\rho) \, r'(\rho)} + \frac{\mu'(r)}{r'(\rho)} - \frac{n''(\rho) \, \mu(r)}{\left[r'(\rho)\right]^{3}}\right) \, \xi(\rho) \right] \frac{d \, U_{2}(\rho)}{d \rho}$$

$$+ \left\{\frac{1}{7} \left[\nabla^{2} \mu(r)\right] \, \xi(\rho) + \frac{\mu(r) \, \xi'(\rho)}{\left[r'(\rho)\right]^{2}} + \left(\frac{2 \, \mu(r)}{r(\rho) \, r'(\rho)} + \frac{\mu'(r)}{r'(\rho)} - \frac{n''(\rho) \, \mu(r)}{\left[r'(\rho)\right]^{3}}\right) \, \xi(\rho) \right\} U_{2}(\rho)$$

$$+ \frac{1M}{5^{2}} \left[\mathcal{E} - V_{3}^{8} (r(\rho))\right] \, \xi(\rho) \, U_{2}(\rho) = 0 \qquad (II-21)$$

Demanding that the coefficient of  $\frac{du_k(x)}{dx}$  equal zero and that the coefficient of  $\frac{d^2u_k(x)}{dx^2}$  equal  $\zeta(x)$  will define  $\zeta(x)$  and x in such a way that equation (II-21) will assume the form of the Schroedinger equation for a static potential.

one finds

$$r'(\rho) = \left[\mu(\rho)\right]^{\frac{1}{2}} \tag{II-22}$$

which defines the relationship between p and r to be

$$\rho = \int_0^{r} \left[ \mu(r) \right]^{-\frac{1}{2}} dr' \qquad (II-23)$$

Then setting

$$\frac{25'(p)\mu(r)}{[n'(p)]^2} + \left(\frac{2\mu(r)}{n(p)n'(p)} + \frac{\mu'(r)}{n'(p)} - \frac{n'(p)\mu(r)}{[n'(p)]^2}\right)5(p) = 0$$

requires that

$$S(p) = \frac{1}{r(p)[\mu(p)]^{\frac{1}{4}}}$$
 (II-24)

Using equations (II-22) and (II-24), equation (II-21) can finally be reduced to

$$\frac{d^{2}U_{k}(\rho)}{d\rho^{2}} - \frac{\ell(\ell+1)u(r)}{r^{2}}U_{k}(\rho) + \frac{t^{2}}{t^{2}}\left[E - V_{s}^{s}(r) + \frac{t^{2}}{2M}u'(r)\left(\frac{u'(r)}{8u(r)} - \frac{1}{r}\right)\right]U_{k}(\rho) = 0$$
(II-25)

which looks like the Schroedinger equation for a static potential.

Since the wave functions  $\mathcal{V}_{\mathcal{L}}(\rho)$  and  $\mathcal{V}_{\mathcal{L}}(r)$  are related by

the matrix elements of any operator A between states  $\psi_{\rho}(\rho)$  and  $\psi_{\rho}(\rho)$  of equation (II-20) are related to those between the corresponding states  $\psi_{\rho}(\rho)$  and  $\psi_{\rho}(\rho)$  of equation (II-25) by

Outside the range of the momentum dependence / () = /

so

$$\frac{1}{2}(r) = \frac{U_2(p)}{r(p)} = \frac{U_2(r)}{r}$$

in that region. Equation (II-23) can be written

$$s = n - r \int_{0}^{R} \left[ u(n) \right]^{-\frac{1}{2}} dn'$$

$$= n - \int_{0}^{R} \left[ 1 - \left[ u(n) \right]^{-\frac{1}{2}} \right] dn'$$

But for / outside the range of the momentum dependence

So out there

$$p = n - \int_{0}^{\infty} \frac{1}{2} - \left[ \mu(n) \right]^{-\frac{1}{2}} dn' = n - \alpha$$
 (II-26)

Define  $R=\rho+q$  everywhere. This reduces to  $R=\rho$  outside the range of the velocity dependence. Define

Then since  $M=d_r$ , equation (II-25) can be rewritten

$$\frac{d^{4}S_{L}(R)}{dR^{2}} - \frac{\ell(R+1)}{R^{2}} \tilde{S}_{L}(R) + \frac{M}{\hbar^{2}} \left\{ \tilde{E} - \left[ V_{S}(R-1) + \frac{\hbar}{M} R(Ln) \left( \frac{\mu(r(R-1))}{r(R-1)} - \frac{1}{R^{2}} \right) \right] - \frac{\hbar^{2}}{2M} \mu(r(R-1)) \left[ \frac{\mu(r(R-1))}{8\mu(r(R-1))} - \frac{1}{r(R-1)} \right] \right\} \tilde{S}_{L}(R) = 0$$
(II-27)

subject to the boundary condition  $\xi(a) = 0$ . This is the Schroedinger equation for the potential enclosed in the square brackets outside of a hard core of radius  $\alpha$ . Outside the range of the momentum dependence,

Starting now with a potential W(R) outside a hard core of radius A and reversing the steps that lead to equation (II-27), one finds that for any function W(r) which is related to the hard core radius A by equation (II-26) one can write

$$\frac{\mu(r)}{r} \frac{d^{2}[r \chi_{2}(r)] - \frac{\ell(R+1)}{R^{2}} \chi_{2}(r) + \nabla \mu(r) \cdot \nabla \chi_{2}(r) + \frac{1}{4} \chi_{2}(r) \nabla \mu(r)}{R^{2} \chi_{2}(r) \left(\frac{\mu(r)}{8\mu(r)} - \frac{1}{r}\right)} \chi_{2}(r) = 0 \qquad (II-28)$$

where

$$R = p + a$$

$$a = \int_{0}^{a} \{1 - [\mu(n)]^{-\frac{1}{2}} \} dr'$$

From equation (II-28) one can deduce a velocity dependent potential which gives identical two-body phase shifts to those produced by the original hard core potential.

Rewriting equation (II-28) as

$$\left\{ \frac{d^{2}}{dr^{2}}r - \frac{\mathcal{L}(Rr)^{2}}{\mathcal{L}(r)R(r)^{2}} + \frac{\mathcal{L}'(r)^{2}}{\mathcal{L}(r)} \frac{d}{dr} + \frac{\mathcal{L}''(r)^{2}}{\mathcal{L}(r)} + \frac{\mathcal{L}'(r)^{2}}{\mathcal{L}(r)} - \left[ \frac{\mathcal{L}'(r)}{\mathcal{L}(r)} \right]^{2} + \frac{k^{2}r}{\mathcal{L}(r)} - \frac{MW(R(r))}{\frac{1}{2}^{2}\mathcal{L}(r)} r \right\} \psi(r) = 0$$
(II-29)

and defining

results in

In order to eliminate the first derivative of  $U_{L}(r)$  , define

which leads to

This can be written in the form of a Schroedinger equation with a static potential

where

$$V(r) = \frac{W(R)}{u(r)} + \frac{\hbar^{2}}{M} \left\{ 2(2+1) \left[ \frac{1}{R(r) \mu(r)} - \frac{1}{r^{2}} \right] + \frac{[\mu(r)-1]}{\mu(r)} k^{2} + \frac{\mu''(r)}{4\mu(r)} - 3 \left[ \frac{\mu'(r)}{4\mu(r)} \right]^{2} \right\}$$
(II-30)

and

$$R(r) = \rho(r) + a$$

$$J(r) = \int_{0}^{r} \left[ \mu(r) \right]^{-\frac{1}{2}} dr$$

$$a = \int_{0}^{r} \left[ 1 - \left[ \mu(r) \right] \right]^{-\frac{1}{2}} dr$$

$$R(r) = \frac{v_{k}(r)}{r \left[ \mu(r) \right]^{\frac{1}{2}}}$$

The potential V(r) is referred to as the Baker transform of the static hard core potential W(r). Any function  $\mu(r)$  which gives the correct value for the hard core radius, q,

defines a new effective potential V(r). Thus a whole family of momentum-dependent potentials can be generated having phase shifts identical to those produced by the hard core potential W(r). Since outside the range of the velocity dependence  $\mu(r)=1$ ,  $\nu_{\lambda}(r)=\nu_{\lambda}(r)$  which is just the usual two body radial wave function. This equivalence of the hard core potential and its Baker transform for the two-body interaction does not imply their equivalence in the many body problem.

### SECTION III

### **POTENTIALS**

The study of the model dependence of nuclear matter was carried out in two parts. The first involved only changes in the potential used in the  $^1\mathrm{S}_0$  state with the  $^3\mathrm{S}_1$ , P, and D states always represented by the Hamada-Johnston potential. In the second part, the changes in the contributions of all of the states were calculated when the Hamada-Johnston potential was replaced by several different momentum dependent potentials having the same on-energy-shell matrix elements as the Hamada-Johnston potential.

The work involving the  $^1\mathrm{S}_0$  state alone was carried out using the potentials shown on Figure 2.5 The three static potentials used are each representative of a family of potentials developed by precisely fitting the  $^1\mathrm{S}_0$  phase shifts obtained from energy independent phase shift analyses of the proton-proton elastic scattering data between 9 MeV and 330 MeV and the pp scattering length. These potentials were constrained to be smooth functions of distance throughout their range, including the region around the edge of the repulsive core. This is in sharp contrast to some of the better known potentials which have large discontinuities at the core edge. The result is that these new potentials are

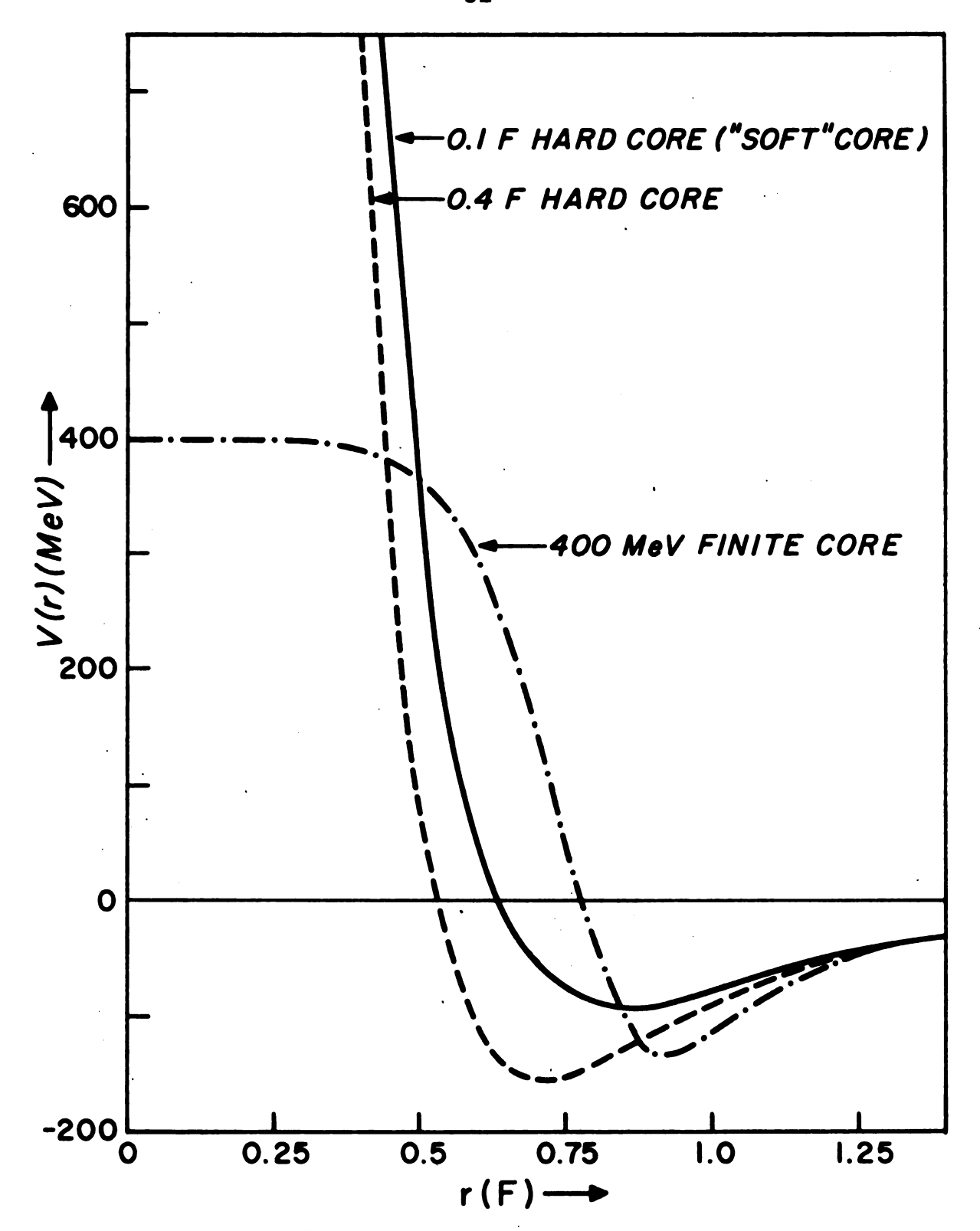


Figure 2. Static <sup>1</sup>S<sub>0</sub> potentials. See Reference 5.

less sensitive to variations in the mesh size around the core edge in numerical calculations.

Potentials were available which had hard cores of radii 0.1 F to 0.4 F and which fit the  $^1{\rm S}_0$  phase shifts equally well. The potential having a hard core radius of 0.1 F was classified as a soft core potential because of its Yukawa repulsion at small distances which joined smoothly onto the hard core at 0.1 F. Presumably the Yukawa repulsion could have been continued into the origin, but it is so large at 0.1 F that there probably would have been little difference in the resulting potential outside 0.1 F.

The 400 MeV finite core potential was one of a group of potentials having core heights ranging from 400 MeV to 2000 MeV. These were generated in the same manner as the hard core potentials. The parameterizations of the three static potentials used here are given below:<sup>5</sup>

Hard core 1S0 potential

$$V(r) = V_{open} - 6.5525 = -1054.7 = +6727.5 = for r > 0.47 = 0$$

"Soft" core <sup>1</sup>S<sub>0</sub> potential

$$V(r) = V_{oper} - 1411.3 \frac{e^{-4x}}{x} + 5281.9 \frac{e^{-7x}}{x}$$
 for  $r > 0.1F$ 

400 MeV finite core 1S0 potential

where

$$X = \frac{M_{\rm IC} \, r}{h \, c}$$
 $\frac{h}{h} = 197.322 \, MeV - F$ 
 $M_{\rm IC} = 197.322 \, MeV - F$ 
 $M_{\rm IC} = 135.0 \, MeV$ 
 $V_{\rm OPER} = -0.08 \, M_{\rm IC} \, \frac{e^{-X}}{X}$ 
 $X_{\rm IC} = 0.78589$ 

The <u>effective</u> momentum-dependent potentials shown in Figure 3 were all obtained from the 0.4 F hard core potential using equation (II-30) and should not be thought of as being completely equivalent to the three static potentials. They may be used in the Schroedinger equation with an effective wave function which agrees with the true wave function only in the region outside the range of the momentum dependence.

The form of 
$$\mu(r)$$
 used here was  $\mu(r) \equiv f(r)$  where  $f(r) \equiv l + (e^n - l) e^{-\frac{nr}{a}}$ ,  $n \geqslant 0$ 

This form is convenient because it allows the integrals involved in calculating  $\nearrow$  (?) and a to be solved analytically, giving

$$p(r) = r - \alpha + \frac{\alpha}{n} \ln(f(r)) = R(r) - \alpha$$

Taking the Baker transform of the 0.4 F hard core potential with u(r) as described above, one finds

$$V(r) = V_{oper} f(r)^{-\frac{X_{A}}{n}} - 6.5525 e^{-2X} f(r)^{-\frac{2X_{A}}{n}}$$

$$-1054.7 e^{-4} f(r)^{-\frac{4X_{A}}{n}} + 6727.5 e^{-\frac{9X_{A}}{n}} \int_{M_{\pi}}^{hc} \frac{hc}{R(r) f(r)}$$

$$+ \frac{n^{4}h^{2} (f(r) - 1) (1 + 4a^{2}k^{2}/n)}{4a^{2} f(r) M}$$
(III-1)

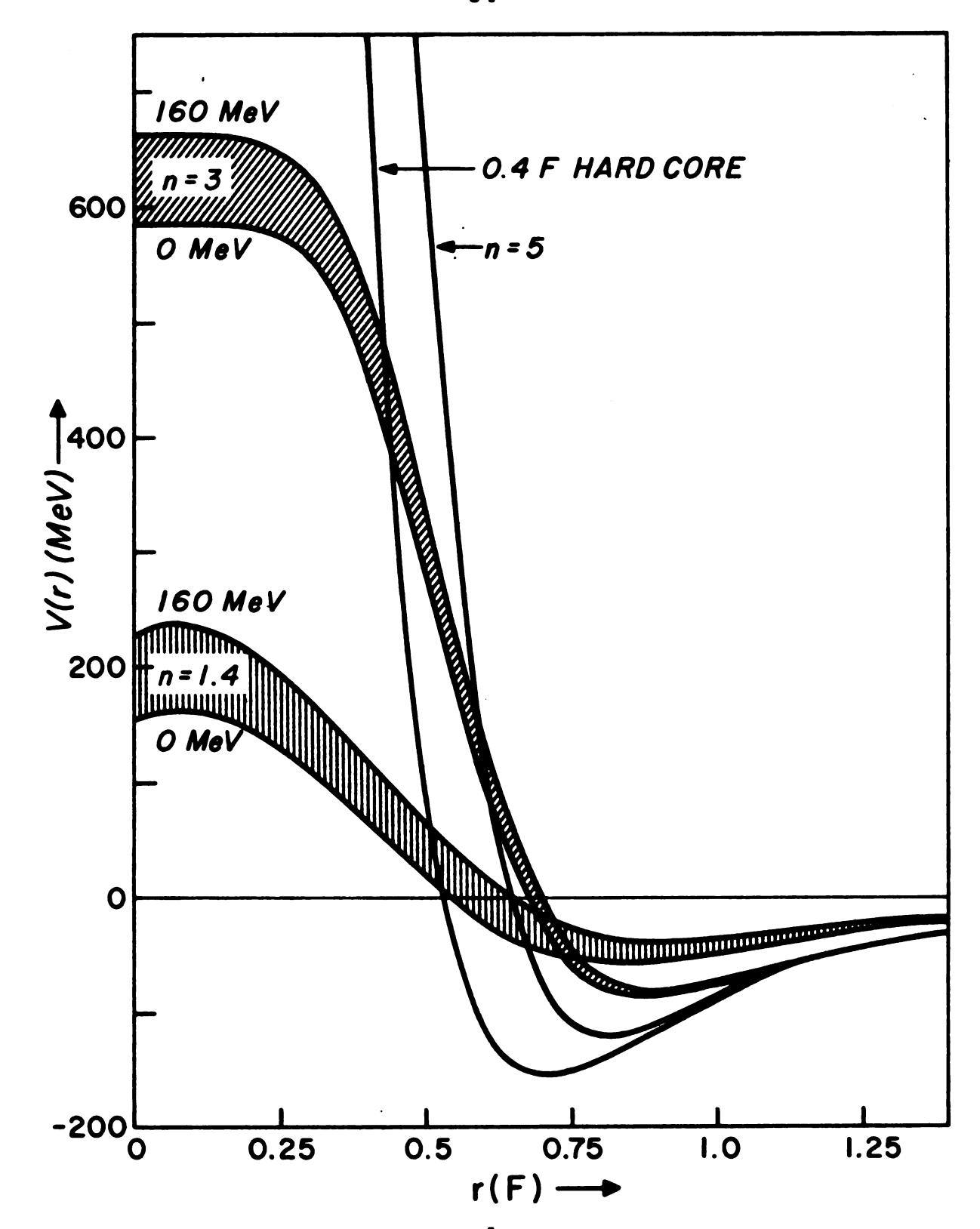


Figure 3. Momentum-dependent  $^{1}S_{0}$  potentials. Generated from 0.4 F hard core potential.

where

$$\chi_{a} = \frac{m_{c} a}{\hbar c}$$

$$R(r) = r + \frac{a}{n} \ln[f(r)]$$

$$a = 0.4F$$

and  $\mathcal{M}$  is the nucleon mass. Care must be taken in treating the coulomb interaction in the effective potential. The coulomb potential must be included in the potential for isospin triplet states before the transformation is made. This results in an additional factor

$$e^{2}f(r) = 1.4399 f(r) = \frac{1.4397}{\mu(r)}$$

which must be added to the term in the square brackets of equation (III-1). The resulting effective potential is the correct one to use for the pp interaction. For nucleon-nucleon interactions which do not involve the coulomb potential one must then subtract

$$\frac{e^2}{r\mu(r)} = \frac{1.4399}{r\mu(r)}$$

from the effective potential for the isospin triplet states. The  $\mu(r)$  in the denominator is required because of the form of the effective potentials and wave functions.

The longest range momentum dependence used in the  $^1\mathrm{S}_0$  state was one in which the range parameter,  $^n$ , in the equation for f(r) was set equal to 1.4. This produced a momentum dependence with the same range as that used in the Bryan-Scott potential for this state. The effective momentum-dependent potential for this value of the range parameter and a shorter-ranged one with the value of the range parameter set at 3 are included in Figure 3. All of

the potentials are in good agreement beyond about 1.4 F, except for the intermediate range momentum-dependent one. It is significantly less attractive than the others beyond about 0.8 F.

For the  $^3\mathrm{S}_1$ , P, and D states there was no set of static potentials comparable to the one available for the  $^1\mathrm{S}_0$  state. Consequently, for these states it was only possible to compare hard core and momentum-dependent potentials. The hard core potential used was the Hamada-Johnston potential which consisted of a sum of four terms:

The subscripts refer to the central, tensor, linear spinorbit, and quadratic spin orbit contributions, respectively. The individual contributions are given by

$$V_{c}(r) = 0.08 \left( \frac{1}{3} m_{R} \right) \left( \vec{r}_{1} \cdot \vec{r}_{2} \right) \left[ 1 + \alpha_{T} \, Y(A) + b_{T} \, Y_{c}^{2}(A) \right]$$

$$V_{cs}(r) = m_{R} \, G_{cs} \, Y_{cs}^{2} \left[ 1 + b_{cs} \, Y(A) \right]$$

$$V_{cc}(r) = m_{R} \, G_{cc} \, X^{-2} \, Z(A) \left[ 1 + a_{cc} \, Y(A) + b_{cc} \, Y_{c}^{2}(A) \right]$$

where

$$\frac{y_{(x)}}{x} = \frac{e^{-x}}{x}$$

$$\frac{z_{(x)}}{x} = \frac{(1 + \frac{3}{x} + \frac{3}{x^2})}{x} \frac{y_{(x)}}{x}$$

$$x = \frac{m_{\pi} n}{h} e$$

The pion mass,  $m_{re}$ , is 139.4 MeV, and the hard core radius is 0.4855 F for all states. The parameters a, b, and c, which are state dependent, are given in Table II. The operators c, c, c, c, and c, are defined by

$$S_{12} = 3 \frac{(\vec{\sigma}_{1} \cdot \vec{r}) (\vec{\sigma}_{2} \cdot \vec{r})}{r^{2}} - (\vec{\sigma}_{1} \cdot \vec{\sigma}_{2})$$

$$\vec{L} \cdot \vec{S} = \frac{1}{4} (\vec{J}^{2} - \vec{L}^{2} - \vec{S}^{2}) = \frac{1}{4} \left[ J(J+i) - L(L+i) - S(S+i) \right]$$

$$L_{12} = (\vec{\sigma}_{1} \cdot \vec{\sigma}_{2}) \vec{L}^{2} - \frac{1}{4} \left\{ (\vec{\sigma}_{1} \cdot \vec{L}) (\vec{\sigma}_{2} \cdot \vec{L}) + (\vec{\sigma}_{1} \cdot \vec{L}) (\vec{\sigma}_{1} \cdot \vec{L}) \right\}$$

$$= \left\{ S_{LJ} + (\vec{\sigma}_{1} \cdot \vec{\sigma}_{2}) \right\} \vec{L}^{2} - (\vec{L} \cdot \vec{S})^{2}$$

Equivalent momentum-dependent potentials were generated from the Hamada-Johnston potential numerically.

Table II. Hamada-Johnston potential parameters.

			· · · · · · · · · · · · · · · · · · ·		
Parameter	Singlet even	Triplet odd	Triplet even	Singlet odd	
a <sub>C</sub>	8.7	-9.07	6.0	-8.0	
b <sub>с</sub>	10.6	3.48	-1.0	12.0	
$\mathtt{a}_{\mathbf{T}}^{}$		-1.29	-0.5		
$\mathtt{b}_{\mathbf{T}}^{}$		0.55	0.2		
$^{\mathtt{G}}_{\mathtt{LS}}$		0.1961	0.0743		
b <sub>LS</sub>		-7.12	-0.1		
${ t G_{LL}}$	-0.000891	-0.000891	0.00267	-0.00267	
a <sub>LL</sub>	0.2	-7.26	1.8	2.0	
$\mathtt{b_{LL}}$	-0.2	6.92	-0.4	6.0	

### SECTION IV

### CALCULATIONS

The binding energy per nucleon to first order in the reaction matrix was calculated using the method described by Brueckner and Masterson (BM) for static potentials and modified as outlined by Ingber for momentum-dependent potentials. The approximations made in BM simplify the calculations considerably, but at the expense of 1 or 2 MeV in the accuracy with which the mean binding energy per nucleon is determined. This does not seriously detract from the usefulness of the method, however, because the main object here is to compare potentials, not to obtain the best possible value from each one. It is more important, in this case, that the same approximations be made for each potential.

## A. Static Potential Calculations

The first step was to calculate the Green's functions for each partial wave. These were obtained by expanding equation (II-17) in partial waves. In order to simplify the calculation of the Green's functions, it was assumed in BM<sup>9</sup> that the energy denominator was independent of the total momentum and was rewritten

$$E_{m} + E_{n} - E_{a}^{*} - E_{l}^{*} = 2[E(k_{ma}) - E^{*}(k_{nl})]$$
 (IV-1)

where  $\mathcal{E}_m$  and  $\mathcal{E}_n$  are the self-consistant energies of particles moving in the Fermi sea and  $\mathcal{E}_a^{\dagger}$  and  $\mathcal{E}_b^{\dagger}$  are the self-consistent energies of excited states above the Fermi sea. The quantity on the right hand side of equation (IV-1) is dependent only on  $k_{m_n}$  and  $k_{4b}$ , the relative momenta of states m and n and states a and b respectively. This approximation is accurate if  $\mathcal{E}_p$  is essentially a quadratic function of  $k_n$  or if the relative momenta are large compared with the total momenta. In line with this approximation, the total momentum was replaced by its average value for a given relative momentum, k, where

$$p^{2} = \frac{6}{5} k_{p}^{2} \left( 1 - \frac{k}{k_{p}} \right) \frac{\left( 1 + \frac{k}{2k_{p}} + \frac{k^{2}}{6k_{p}^{2}} \right)}{\left( 1 + \frac{k}{2k_{p}} \right)} \quad \text{for } k < k_{p}$$

$$= 0 \quad \text{for } k \ge k_{p} \quad \text{(IV-2)}$$

The Green's functions were then given by

$$G_{2}(r,r') = \frac{1}{2\pi^{2}} \int \frac{k^{-2}dk^{0}j_{k}(k^{*}r)j_{k}(k^{*}r')}{2[E(k)-E^{*}(k^{*})]} f(r,k^{*})$$
(IV-3)

for on-energy shell propagation. For off-energy-shell propagation the denominator of the integrand was replaced by  $2\left[\mathcal{E}(k)-\mathcal{E}^*(k')\right]-\Lambda$  where  $\Delta$  is the mean excitation energy, taken to be  $\mathcal{E}(k_r)-\mathcal{E}(0)$ . The Pauli step function, f(P,k''), excluded values of k'' which corresponded to filled states in the Fermi sea. It was given by 20

$$f(P, K') = 0 , (K'^{2} + \frac{1}{2}P^{2})^{\frac{1}{2}} < k_{F}$$

$$= 1 , K'' - \frac{1}{2}P^{2} > k_{F}$$
 (IV-4)
$$= \frac{K'^{2} + \frac{1}{2}P^{2} - k_{F}^{2}}{k^{2}P}$$
 otherwise,

where  $\rho$  is the average momentum of equation (IV-2). In the actual calculation the integral of equation (IV-3) was split into two parts:

$$\frac{1}{2\pi^2}\int_0^{\infty} \cdots = \frac{1}{2\pi^2}\int_0^{k_{IMT}} \cdots + \frac{1}{2\pi^2}\int_{k_{IMT}}^{\infty} \cdots$$

where  $k_{MT}$  was chosen so that the denominator of the integrand could be approximated by  $\frac{\hbar^2 k''}{M}$  for  $k'' > k_{MT} > k_{P}$ . For  $k'' > k_{P}$ , f(P, k'') = 1, so the second part of the integral could be written

But this could be rewritten without further approximation as

$$-\frac{M}{2\pi^{2}k^{2}}\int_{j_{R}}^{\infty}(k''n')j_{R}(k''n')dk'' = -\frac{M}{2\pi^{2}k^{2}}\int_{0}^{\infty}j_{R}(k''n')j_{R}(k''n')dk'' + \frac{M}{2\pi^{2}k^{2}}\int_{0}^{\infty}j_{R}(k''n')j_{R}(k''n')dk''$$

The first integral on the right side was evaluated analytically, giving for on-energy-shell propagation

$$G_{2}(n,n') = -\frac{M}{4\pi n \, \hbar^{2}(2l+1)} \left(\frac{n_{c}}{r_{c}}\right)^{l} + \frac{1}{2\pi^{2}} \int_{J_{2}}^{J_{2}} (k^{n}n) j_{2}(k^{n}n') \left\{\frac{M}{\hbar^{2}} + \frac{k^{n^{2}} f(p,k'')}{2[E(k)-E^{2}(k'')]}\right\} dk''$$
(IV-5)

where r is the lesser and r, the greater of r and r'.

The wave functions were calculated by iteration of the equation

where  $V_{ll''}^{J_l}(r')$  is the static two body potential and

$$S_{2}(kr) = \frac{j_{2}(kr) - \left[ \frac{j_{2}(kr_{c})}{g_{2}(r,r_{c})} \right] / \left( \frac{g_{2}(r,r_{c})}{g_{2}(r,r_{c})} \right]}{F_{2}(r,r_{c}) = \frac{g_{2}(r,r_{c}) - \left[ \frac{g_{2}(r,r_{c})}{g_{2}(r,r_{c})} \right] / \left( \frac{g_{2}(r,r_{c})}{g_{2}(r,r_{c})} \right) / \left( \frac{g_{2}(r,r_{c})}{g_{2}(r,r_{c})} \right) }$$

The forms of  $S_{\ell}$  and  $F_{\ell}$  resulted from the requirement that the wave function vanish at  $P_{\ell}$ , the radius of the hard core. For potentials having no hard core,

The wave function in the integrand of equation (IV-6) was initially set equal to  $S_{LL'}$ . Thereafter the values of the wave functions calculated on the previous iteration were used in the integrand. This was repeated until for any value of P the change in the wave function on two successive iterations was smaller by at least a factor of  $10^{-3}$  than the wave function itself.

The reaction matrix elements were then calculated using

$$\langle k|K/k\rangle = \sum_{J_{S}} \sum_{\ell=J-1}^{J_{H}} C_{J_{\ell}S} \left[ -\frac{j_{R}^{\lambda}(k_{\ell})}{\varsigma_{R}(k_{\ell},k_{\ell})} + 4_{J_{L}} \int_{k_{\ell}}^{\infty} dr \, \varsigma_{R}(k_{\ell}) \sum_{\ell=J-1}^{J_{H}} V_{L_{R}}(r) \, V_{L_{R}}(k_{\ell},r) \right]$$

$$+ 4_{J_{L}} \int_{k_{\ell}}^{\infty} dr \, \varsigma_{R}(k_{\ell}) \sum_{\ell=J-1}^{J_{L}} V_{L_{R}}(r) \, V_{L_{R}}(k_{\ell},r)$$

$$(IV-7)$$

where

$$C_{Jes} = \frac{(2J+i)(2T+i)}{3}$$

J is the total angular momentum and T is the isospin. For potentials which do not have a hard core, the first term in the square brackets is zero.

Finally, the single particle potential was calculated from

$$V(k) = \frac{6}{\pi^{2}} \int_{0}^{\infty} k'^{2} dk' \langle k' | K | k' \rangle$$

$$+ \frac{3}{\pi^{2}} \int_{0}^{\infty} k'^{2} dk' \langle k' | K | k' \rangle \left( 1 + \frac{k_{0}^{2} - k^{2} - 4k'^{2}}{4kk'} \right)$$

$$|k_{e} - k|_{2}^{2}$$
(IV-8)

for  $k < k_p$ . For  $k \ge k_p$  the first integral vanishes. These single particle potentials were then used in recalculating the energy denominators of the Green's functions given by equation (IV-5)

Starting with these new Green's functions, a new set of single particle potentials was calculated. This process was repeated until the single particle potentials used in

calculating the Green's functions reappeared in equation (IV-8). When these self-consistent single particle potentials had been obtained, the mean binding energy per nucleon was calculated from

$$E = \frac{3}{k_{\mu}^{3}} \int_{0}^{k_{\mu}} k^{2} dk \left[ \frac{k^{2}k^{2}}{2M} + \frac{1}{2} V(k) \right]$$

The saturation density is determined by finding the Fermi momentum for which the mean binding energy reaches a minimum. The saturation density was not calculated here. Instead the Fermi momentum was fixed at its experimental value of  $1.4 \, \text{F}^{-1}$ .

# B. Momentum-Dependent Potential Calculations

In order to treat momentum-dependent potentials, equations (IV-6) for the wave function and (IV-7) for the reaction matrix elements had to be modified. For a momentum-dependent potential,  $\bigvee_{k,l}^{\mathcal{J}_k}(\mathcal{P}_{r,l},r)$ , these equations become

and

Both of these equations now involve derivatives of the wave function. These are difficult to calculate because the wave function is calculated numerically by an iterative process. However, by integrating equations (IV-9) and (IV-10) by parts, it is possible to eliminate the wave function

derivatives in favor of derivatives of Bessel functions and Green's functions, both of which can be expressed analytically. 19

In order to carry out this modification it was necessary to know something about the form of the potential,  $\bigvee_{l,r}^{J_s}(\mathcal{P}_{r,r})$ . Defining a function

$$\omega(r) = \frac{1}{2} \left( \mu(r) - 1 \right)$$

the Schroedinger equation for a momentum-dependent potential, equation (II-18), can be rewritten

$$\frac{\sum p^2}{M} + \frac{\omega(r)p^2 + p^2\omega(r)}{M} + \sqrt{2}(r) \frac{2}{3} \psi(r) = E\psi(r) \qquad (IV-11)$$

where

$$V_s(r) \equiv V_s(r) + \frac{4^3}{M} \left( \frac{\omega'(r)}{r} + \frac{\omega''(r)}{2} \right)$$

is the static part of the potential. The quantity  $\omega(r)$  will in general be a function of  $\mathcal{J}$ ,  $\mathcal{L}$ , and s. However, for convenience, these subscripts as well as those on  $\mathcal{L}(r)$  and  $\mathcal{L}(r)$  will be suppressed. In the actual calculations the same  $\omega(r)$  was used for all states, although there is certainly no reason to expect this to be true. This will be discussed in greater detail later.

The term  $\binom{b}{s}(r)$  in the static part of the potential in equation (IV-11) can be evaluated by comparing equations (II-20) and (II-29) with the result

Using  $\mu(r) = /+ 2\omega(r)$  and  $\mu'(r) = 2\omega'(r)$  this becomes

$$V_{s}(r) = W_{\ell,\epsilon'}^{J_{s}}(R(r)) + \frac{\hbar^{2}}{M} \left\{ \ell(\ell+1) \left[ \frac{1}{R_{\ell,r}^{2}} - \frac{1+2\omega(r)}{r^{2}} \right] + \omega'(r) \left[ \frac{\omega'(r)}{4[1+2\omega(r)]} - \frac{1}{r} \right] \right\}$$

So ((r) can be written

$$V_{s}(r) = W_{RR'}(R(r)) + \frac{t^{\Delta}}{M} \left\{ R(l+1) \left[ \frac{1}{R^{2}(r)} - \frac{1+2\omega(r)}{r^{\Delta}} \right] + \frac{\left[\omega'(r)\right]^{2}}{4\left[1+2\omega(r)\right]} + \frac{\omega''(r)}{2} \right\}$$

$$= W_{RR'}^{J_{s}}(R(r)) + W_{0}(r) - \frac{2l(l+1)t^{\Delta}\omega(r)}{Mr^{\Delta}}$$

From equation (IV-11) it is clear that

$$V_{RR'}^{J_s}(\nabla_r, r) = \frac{\omega(r)\rho^2 + \rho^2 \omega(r)}{M} + V_s(r)$$
 (IV-13)

This can be expressed in a form that is more convenient for use in equations (IV-9) and (IV-10). Multiplying on the right by  $\binom{r}{k_{\ell}}(k_{\ell})$  and carrying out the operations implied by the momentum operators in  $\binom{r}{k_{\ell}}(r_{r},r)$ , equation (IV-13) becomes

$$V_{ee}^{J_{s}}(V_{r},r) \stackrel{1}{\not\sim} (k,r) = \left\{ V_{s}(r) + \frac{h^{2}}{M} \left[ \frac{2\ell(\ell+1)}{r^{2}} \omega(r) - \frac{2\omega'(r)}{r} - \omega''(r) \right] \right\} \stackrel{J_{s}}{\not\sim} (k,r)$$

$$- \frac{h^{2}}{M} \left[ \frac{4\omega(r)}{r} + 2\omega'(r) \right] \frac{d}{dr} \stackrel{J_{s}}{\not\sim} (k,r)$$

$$- \frac{2h^{2}}{M} \omega(r) \stackrel{d}{\not\sim} \stackrel{J_{s}}{\not\sim} (k,r)$$

$$(IV-14)$$

for the uncoupled states. This can be rewritten

where

$$\alpha(r) = W_0(r) - \frac{h^2}{M} \left[ \frac{2\omega'(r)}{r} + \omega''(r) \right]$$
 (IV-16)

$$\beta(r) = -\frac{2 \frac{\pi^2}{M} \left[ \frac{2 \omega(r)}{r} + \omega'(r) \right] \qquad (IV-17)$$

$$\gamma(r) = -\frac{2\hbar^2}{M}\omega(r) \tag{IV-18}$$

If coupled states are to be included, this becomes

$$\sum_{k''} V_{kk''}(Q_{\rho_{i}} r) \psi_{kk''}^{J_{a}}(k_{i} r) = \sum_{k'} W_{k'k'}(R_{i} r) \psi_{kk''}^{J_{a}}(k_{i} r)$$

$$+ \sum_{k''} \alpha(r) + \beta(r) \frac{d}{dr} + \gamma(r) \frac{d^{a}}{dr^{a}} \left\{ \psi_{kk'}^{J_{a}}(k_{i} r) \right\}$$

$$(IV-19)$$

Using this expression in equation (IV-9) and integrating by parts, the wave function becomes

where

$$A(r) = \alpha(r) + \frac{2}{r} \chi(r) + \frac{7}{r} \chi'(r) + \chi''(r) - \frac{1}{r} \beta(r) - \beta'(r)$$

$$B(r) = \frac{7}{r} \chi(r) + 2\chi'(r) - \beta(r)$$

The second derivative of the Green's function can be eliminated by using

From which one obtains

So

Which can be rewritten

$$[1+2\omega(r)]_{ZR}^{J_{0}}(k,r) = j_{R}(kr) \delta_{RR}^{J_{0}} + 4\pi \int_{0}^{\infty} n^{3} dr' \left\{ \sum_{R''} W_{R'R''}(R(n)) \right\}_{RR''}^{J_{0}}(n')$$

$$+ \frac{1}{2} \sum_{RR''} (k,r') \left[ W_{0}(n') + \frac{1}{2} (2k^{2}\omega(n') - \frac{1}{2}\omega'(n') - \omega''(n') \right]$$

$$- 2\omega'(n') \frac{d}{dn'} \right] G_{R''}(n,n') \qquad (IV-20)$$

On the first iteration the value of the wave function in the integrand was taken to be

In order to evaluate equation (IV-20) it is still necessary to know  $\frac{1}{dr}G_{\ell}(r,r)$  . For on-energy-shell propagation

$$\frac{d}{dr'} G_{2}(r,r') = \frac{1}{2\pi^{2}} \int_{0}^{\infty} \frac{dk'' j_{2}(k''n) \frac{d}{dr'} j_{2}(k''n') f(P,k'')}{2[E(k) - E^{*}(k'')]}$$

$$= \frac{1}{2\pi^{2}} \int_{0}^{\infty} \frac{k''' dk'' j_{2}(k''n') \frac{d}{dr'} j_{2}(k''n') - k'' j_{2r'}(k''n')}{2[E(k) - E^{*}(k'')]} f(P,k'')$$

with  $2[C(\lambda)-C^*(\lambda'')]+\Delta$  in the denominator for off-energy-shell propagation. The derivative of the Green's function was calculated in a manner similar to that used for the Green's function itself. In this case the result was

$$\frac{d}{dr'} G_{2}(r,r') = \frac{1}{2\pi L} \int_{0}^{k_{MT}} J_{2}(k''r) \left[ \frac{R}{r'} J_{2}(k''r') - k''_{2k+1}(k''r') \right] \left\{ \frac{M}{h^{L}} + \frac{k''^{2} f(P,k'')}{2[E(k) - E''(k'')]} \right\} dk'' \\
- \frac{M}{2\pi^{2}h^{2}} \left\{ \frac{R\pi}{2R^{M}(2R^{N})} \left( \frac{R}{r_{2}} \right)^{2} - \frac{\pi}{2\pi^{12}} \left( \frac{r}{r''} \right)^{2} U(r''-r) \right\} \qquad (IV-21)$$

where  $r_{\zeta}$  is the lesser and  $r_{\zeta}$  the greater of  $r_{\zeta}$  and  $r_{\zeta}$ , and  $r_{\zeta}$  is a step function defined by

$$U(r'-r) = 1, \text{ if } r'>r$$

$$\frac{1}{4}, \text{ if } r'=r$$

$$0, \text{ if } r'$$

The equation for the reaction matrix elements was also integrated by parts to eliminate the derivatives of the wave function. In this case recursion relations were used to eliminate the second derivative of the Bessel function leaving

$$\langle k/K/k \rangle = \frac{4\pi h}{M} \sum_{J_{2}} \sum_{L_{2}J_{-1}}^{J_{1}} c_{J_{2}} \int_{r}^{r} dr \left\{ \sum_{k=J_{-1}}^{J_{1}} \frac{M}{h} \frac{1}{k_{k}} (k,r) W_{kl}^{J_{2}} (R(r)) j_{k}(kr) + \frac{1}{k_{k}} (k,r) \left[ \frac{M}{h} W_{0}(r) - (2l(l+1) - 2k^{2}r^{2}) w(r) - 2r(l+1) w'(r) \right] - r^{2} w'(r) \left[ j_{k}(kr) + 2k w'(r) \frac{1}{k_{k}} (k,r) j_{kr}(kr) \right]$$

$$(IV-22)$$

With these changes it was possible to extend the method described in BM to momentum-dependent potentials. Because of the necessity of calculating the first derivative of the Green's function and the need to extend the region of integration all the way in to the origin instead of just to the hard core radius (0.4 F to 0.5 F usually), the computer time required for momentum-dependent potentials was about two to four times as great as that required for hard core potentials.

		:

## C. Phase Shift Calculation

As a check on the validity of the equations and the programing, one further modification was made in the equations for the momentum-dependent potentials. By changing the denominator of the Green's functions and their derivatives (equations(IV-5) and (IV-21)) to be just the difference of the relative kinetic energies

and setting f(P, k'') = 1 for all P and k'', the Green's functions and their derivatives for nuclear matter became those associated with the free two-nucleon elastic scattering problem. The singularity within the range of integration results in complex Green's functions and therefore complex wave functions. From the equations thus modified, the phase shifts,  $\frac{2\pi N}{3}$ , for the uncoupled states could be calculated using

and compared with the known values of those phase shifts. The integrand of equation (IV-23) is of the same form as that of equation (IV-10) which was evaluated as shown in equation (IV-22).

### SECTION V

### RESULTS

Before using the program to calculate the binding energy of nuclear matter, the Green's functions were modified as described previously so that the elastic scattering phase shifts could be calculated. When these were compared with their known values they were found to differ in the third significant figure. This difference was due almost entirely to the method of evaluating the Green's function integral around the singularity. When the free two-nucleon Green's function integral was evaluated analytically, the phase shifts calculated by the two methods were in even better agreement.

Returning to nuclear matter calculations, the Hamada-Johnston hard core potential was used for all states in order to find the self-consistent single particle potential and the binding energy per nucleon predicted by this model for a Fermi momentum of 1.4  $F^{-1}$ . The resulting binding energy per nucleon, 8.5 MeV, is fairly typical of the values predicted by hard core potentials which fit the elastic scattering data and is clearly in poor agreement with the empirical value of 16 MeV. The study of the model dependence of the  $^{1}S_{0}$  state was then carried out using this single particle

potential as a starting point. The Hamada-Johnston  $^1\mathrm{S}_0$  potential was replaced by the O.4 F and O.1 F hard core potentials, the 400 MeV finite core potential, and finally the momentum-dependent  $^1\mathrm{S}_0$  potentials. The results are shown in Table III. From the calculations involving the three static potentials, it was clear that the contributions of the  $^3\mathrm{S}_1$ , P, and D states were not significantly affected by the changes introduced in the single particle potential as a result of using different  $^1\mathrm{S}_0$  potentials. Consequently it was not necessary to recalculate these states when the momentum-dependent  $^1\mathrm{S}_0$  potentials were used.

The results shown in Table III confirm the expectation that potentials having soft cores, finite cores, or a momentum-dependent repulsion all would produce a desirable increase in the binding energy above that predicted by a longer range hard core potential, at least for the 150 state. The maximum amount of binding occurred with the momentumdependent potential having the range parameter about equal to 3. This can perhaps be understood by comparing the effective potentials for n=1.4, 3, and 5, as shown in Figure As the value of the range parameter, n, increases, the size of the short range repulsion increases. This is accompanied by a corresponding increase in the intermediate range attraction. As n increases past 3, the increase in attraction in the intermediate range is not sufficient to counteract the increased short range repulsion seen by the wave function. Similarly as n decreases from 3 down to 1.4,

Table III. Mean binding energy per nucleon predicted by the  $^{1}\mathrm{S}_{0}$  potentials.

1s <sub>0</sub> potential	Potential energy for $^1\mathrm{S}_0$	Total energy * (MeV)
0.4 F hard core	-15.8	-9.3
0.1 F hard core	-16.8	-10.3
400 MeV finite co	re -17.2	-10.7
n=1.4 momentum de	-17. <b>4</b>	-10.9
n=3 momentum dep.	-18.2	-11.7
n=4 momentum dep.	-17.8	-11.3

<sup>\*</sup>Using Hamada-Johnston potential for all other states and including a kinetic energy of 24.39 MeV per nucleon.

very little short range repulsion remains, but there is also virtually no attraction in the intermediate region. This is borne out by Table IV which compares the values of the <sup>1</sup>S<sub>0</sub> reaction matrix elements for each potential to the values obtained when the 0.4 F hard core potential was used. In all cases the gain in the size of the reaction matrix elements increases with momentum, indicating that the size of the short range repulsion is the dominant factor. The momentum-dependent potential with n=1.4 is especially interesting. Although at high momenta the K matrix elements are considerably larger than those of the 400 MeV finite core potential, at small momenta they are somewhat smaller. This seems to verify the previous remark regarding what appears to be an undesirably weak attraction in the intermediate region of this potential.

The 2.4 MeV increase in the average binding energy per nucleon of the  $^1\mathrm{S}_0$  state for the n=3 momentum-dependent potential over the value obtained with the 0.4 F hard core potential is a change in the right direction. But combined with the hard core Hamada-Johnston potential for the other states it still leaves the total of the contributions of all the states short of the 16 MeV empirical value. This clearly indicates the necessity of examining the effects of the various potential forms on the other states.

Table V shows the contribution of each state to the binding energy of nuclear matter for several momentum-dependent potentials and for the Hamada-Johnston potential

Table IV. Percent increase of <sup>1</sup>S<sub>0</sub> K matrix elements over values obtained with 0.4 F hard core potential.

Potential k/k <sub>F</sub> =	0.1	0.3	0.5	0.7	0.9
0.1 F hard core	4.1	5.0	6.3	9.3	17.7
400 MeV finite core	5.7	6.8	8.8	13.1	27.2
n=1.4 momentum dep.	4.7	6.1	9.7	18.8	47.1
n=3 momentum dep.	9.0	11.1	15.2	24.2	50.8

Table V. Mean binding energy per nucleon predicted by momentum-dependent potentials generated from the Hamada-Johnston potential.

State	Hard	Momentum-dependent H-J				
	core H-J (MeV)	n=1.4 (MeV)	n=3 (MeV)	n=5 (MeV)		
<sup>1</sup> s <sub>0</sub>	-15.09	-16.30	-19.66	-20.08 <sup>a</sup>		
<sup>3</sup> s <sub>1</sub>	-16.05	-12.94	-19.55	-21.21 <sup>a</sup>		
<sup>1</sup> <sub>P</sub> <sub>1</sub>	3.68	3.21	3.53	3.61		
<sup>3</sup> P <sub>0</sub>	-3.47	-3.71	-3.69	-3.65		
<sup>3</sup> <sub>P</sub> <sub>1</sub>	11.13	10.07	10.40	10.41		
<sup>3</sup> P <sub>2</sub>	-7.13	-4.73	-7.45	-8.91		
<sup>1</sup> D <sub>2</sub>	-3.09	-2.86	-3.07	-3.11		
<sup>3</sup> D <sub>1</sub>	1.57	1.56	1.57	1.57		
<sup>3</sup> D <sub>2</sub>	-4.47	-4.40	-4.48	-4.48		
Total <sup>b</sup>	-8.54	-6.64	-16.61	-18.69		

<sup>&</sup>lt;sup>a</sup>These values are for n=3.7.

bTotal for each column is the sum of the S states from that column, the P and D states from the hard core H-J column, and a kinetic energy of 24.39 MeV per nucleon.

from which they were generated. The increase in the binding energy of the 15, state when the hard core in that state was replaced by a momentum-dependent repulsion was greater than that obtained when the 0.4 F hard core was replaced by a momentum-dependent repulsion. The  ${}^{3}S_{1}$  state shows even more sensitivity to the form of the short range repulsion than the 1s<sub>0</sub> state. The intermediate range momentum dependence produced about 3 MeV less binding in the  $^3\mathrm{S}_1$  state than the hard core Hamada-Johnston potential. The short range momentum dependence characterized by n=3.7 produced about a 5 MeV increase in binding. Combined with the increase of 5 MeV in the 1S<sub>0</sub> state and using the hard core Hamada-Johnston potential for the P and D states, the n=3.7 momentum dependence in the  ${}^{3}S_{1}$  state produced too much binding. This could be corrected by adjusting the value of the range parameter for either or both of the S states to reduce the binding energy to the desired value. Setting n=3 for both states results in good agreement with the empirical value. event, a deviation of 1 or 2 MeV from the empirical value is not a cause for concern since the method used in the calculation could have introduced errors of this magnitude.

The D states showed some loss of binding with the intermediate range momentum dependence. With the shorter range momentum dependence, n=3, the contribution of these states to the binding energy was brought into close agreement with the values obtained from the hard core potential. This was

perhaps to be expected since the D waves see virtually nothing of the interior region of the potential. What is seen, however, is the decrease in attraction in the intermediate region of the n=1.4 momentum-dependent potential and the fairly close agreement between the hard core and the shorter range momentum-dependent potentials in the intermediate region as shown in Figures 4, 5, and 6. Thus it makes little difference whether a hard core or short range momentum-dependent potential is used in the D states.

The  ${}^{1}P_{1}$ ,  ${}^{3}P_{0}$ , and  ${}^{3}P_{1}$  states together are about 1.8 MeV more attractive when the n=1.4 momentum dependence is used to replace the hard core. This increase in binding is reduced to half this value when the range parameter is set equal to 5. The  ${}^{3}P_{2}$  state more than cancels the increase in binding produced by the other P states for n=1.4. For that value of the range parameter, the <sup>3</sup>P<sub>2</sub> state produces 2.4 MeV less attraction than it does with the hard core potential. This changes to about 1.8 MeV of added attraction when n is increased to 5. As n increases above 5, the increase in attraction levels off and will then gradually return to the value obtained with the hard core potential. Setting the range parameter equal to 3 for all of the P states results in 1.4 MeV more binding energy than is obtained when the hard core Hamada-Johnston potential is used.

The  $^{3}P_{0}$  phase shift is very poorly defined by experiment at energies between about 60 MeV and 130 MeV, a region which

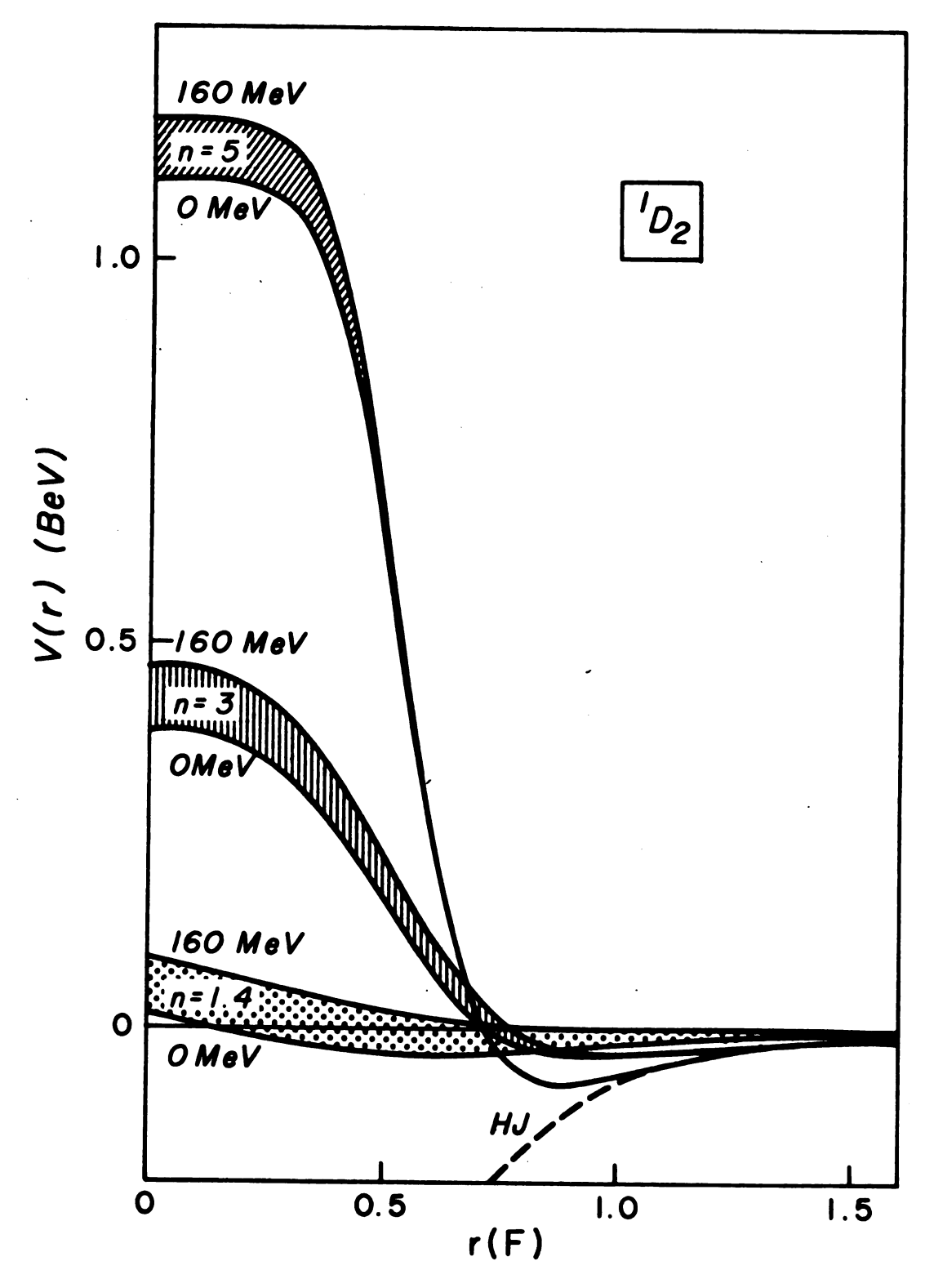


Figure 4. Momentum-dependent  $^{1}\mathrm{D}_{2}$  potentials. Generated from the Hamada-Johnston potential.

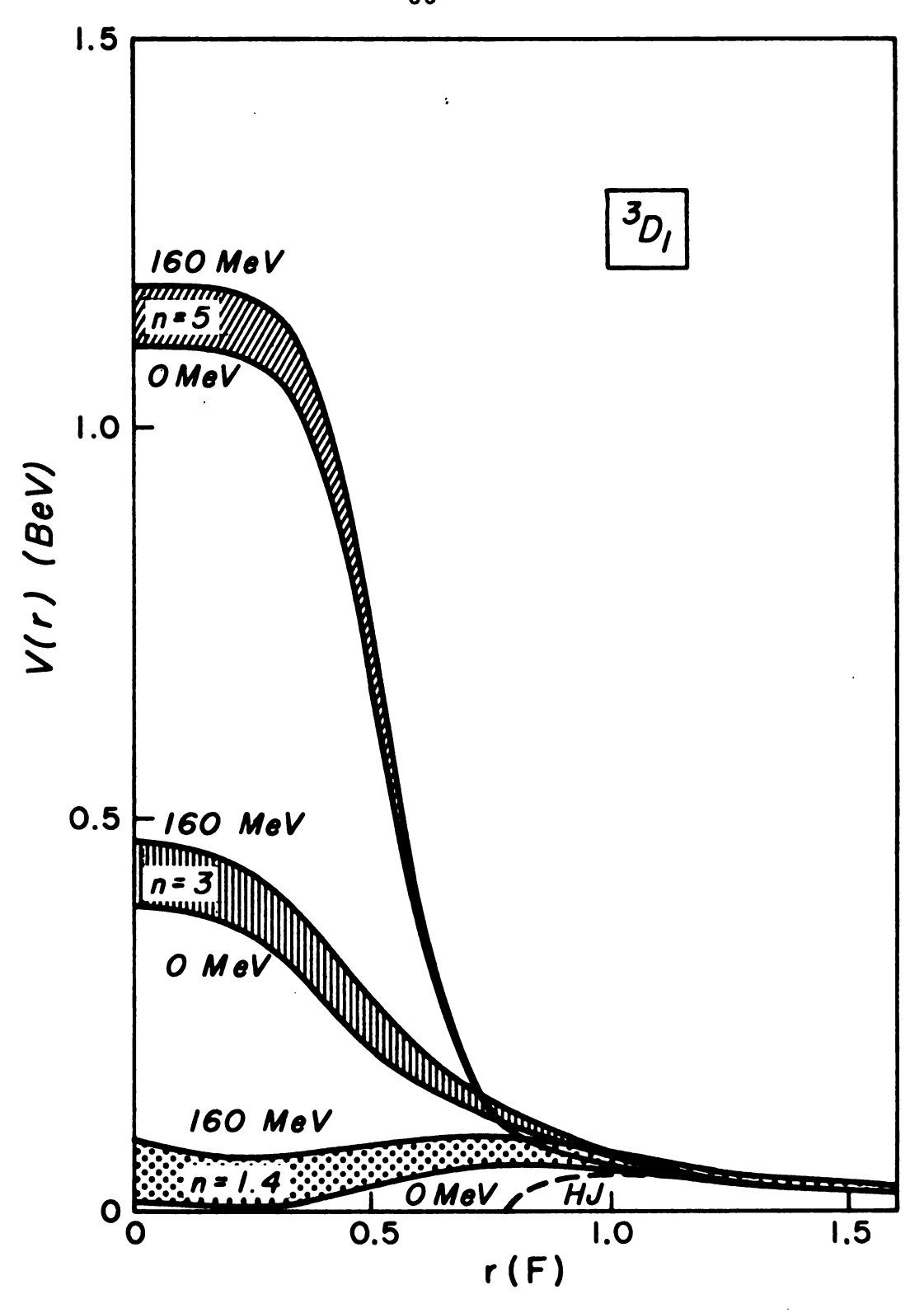


Figure 5. Momentum-dependent  $^3\mathrm{D}_1$  potentials. Generated from the Hamada-Johnston potential.

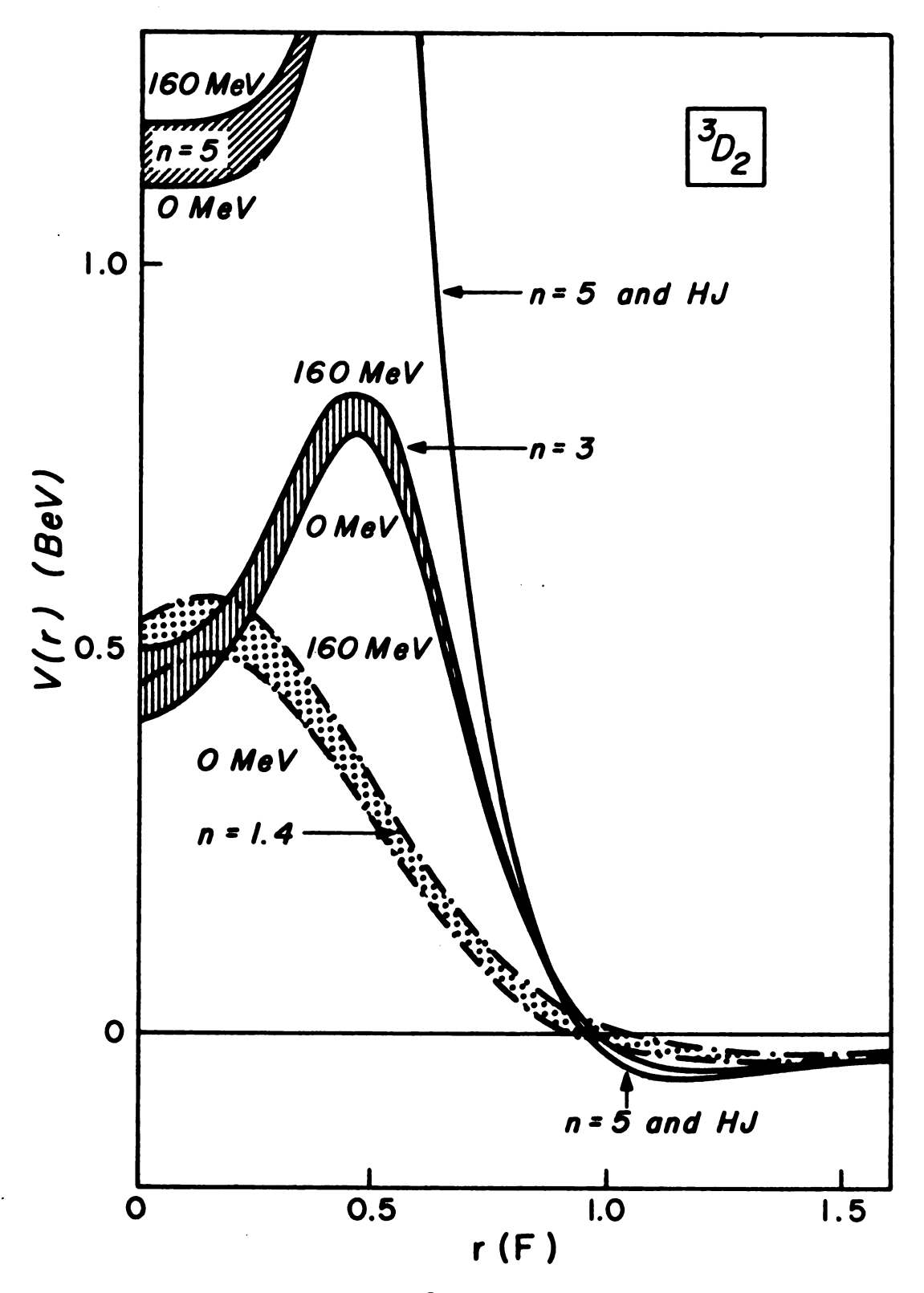


Figure 6. Momentum-dependent  $^{3}\mathrm{D}_{2}$  potentials. Generated from the Hamada-Johnston potential.

is very important in nuclear matter. The uncertainty in this phase shift results in an uncertainty of about 0.4 MeV per nucleon in the contribution of this state to the binding energy of nuclear matter. The  $^3P_1$  and  $^3P_2$  phase shifts are pinned down somewhat better than the  $^3P_0$ , but at energies above about 100 MeV the Hamada-Johnston potential does a rather poor job of fitting these phase shifts. Using the phase shift approximation for the reaction matrix, the Hamada-Johnston potential was found to produce about 0.4 MeV per nucleon less binding than the experimentally determined phase shifts in the  $^3P_0$  state and 0.6 to 0.8 MeV per nucleon more binding in each of the other states. Consequently the numerical results obtained for the P states should be interpreted with caution.

In conclusion, the binding energy of nuclear matter seems to be quite sensitive to the form of the short range repulsion used in phenomenological two-nucleon potentials. Even two-nucleon potentials which have identical on-energy-shell matrix elements may predict mean binding energies per nucleon for the S and P states which differ by several MeV. The binding energies of both the S and the P states showed a desirable increase when a hard core potential was replaced by a short range momentum-dependent one. Using a momentum-dependent potential for the S states and a hard core potential for the P and D states resulted in a mean binding

 $<sup>^{\</sup>star}$ See Figures 7 through 10.

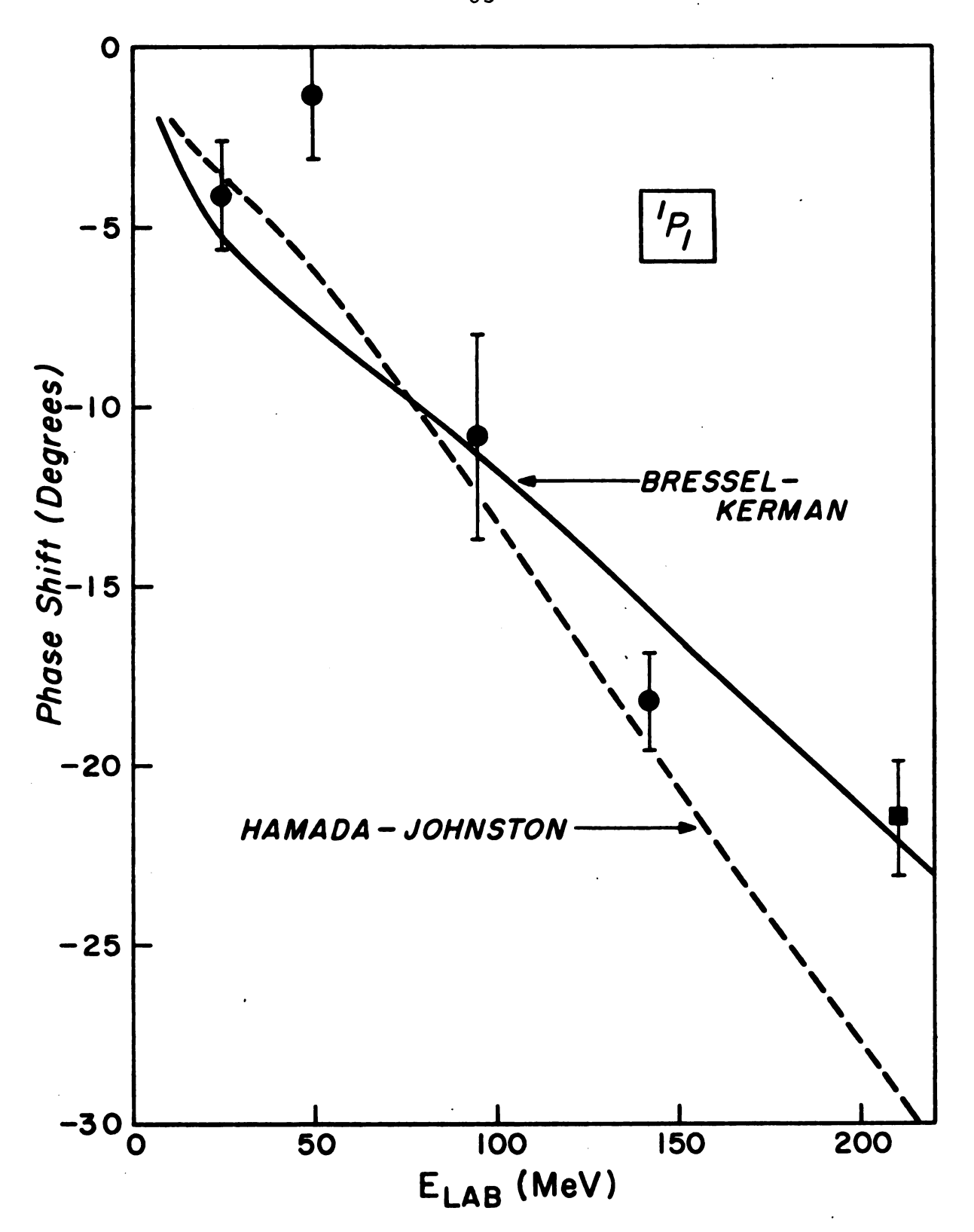


Figure 7. <sup>1</sup>P<sub>1</sub> phase shift vs. energy. Circles are from Reference 22, Squares from Reference 4.

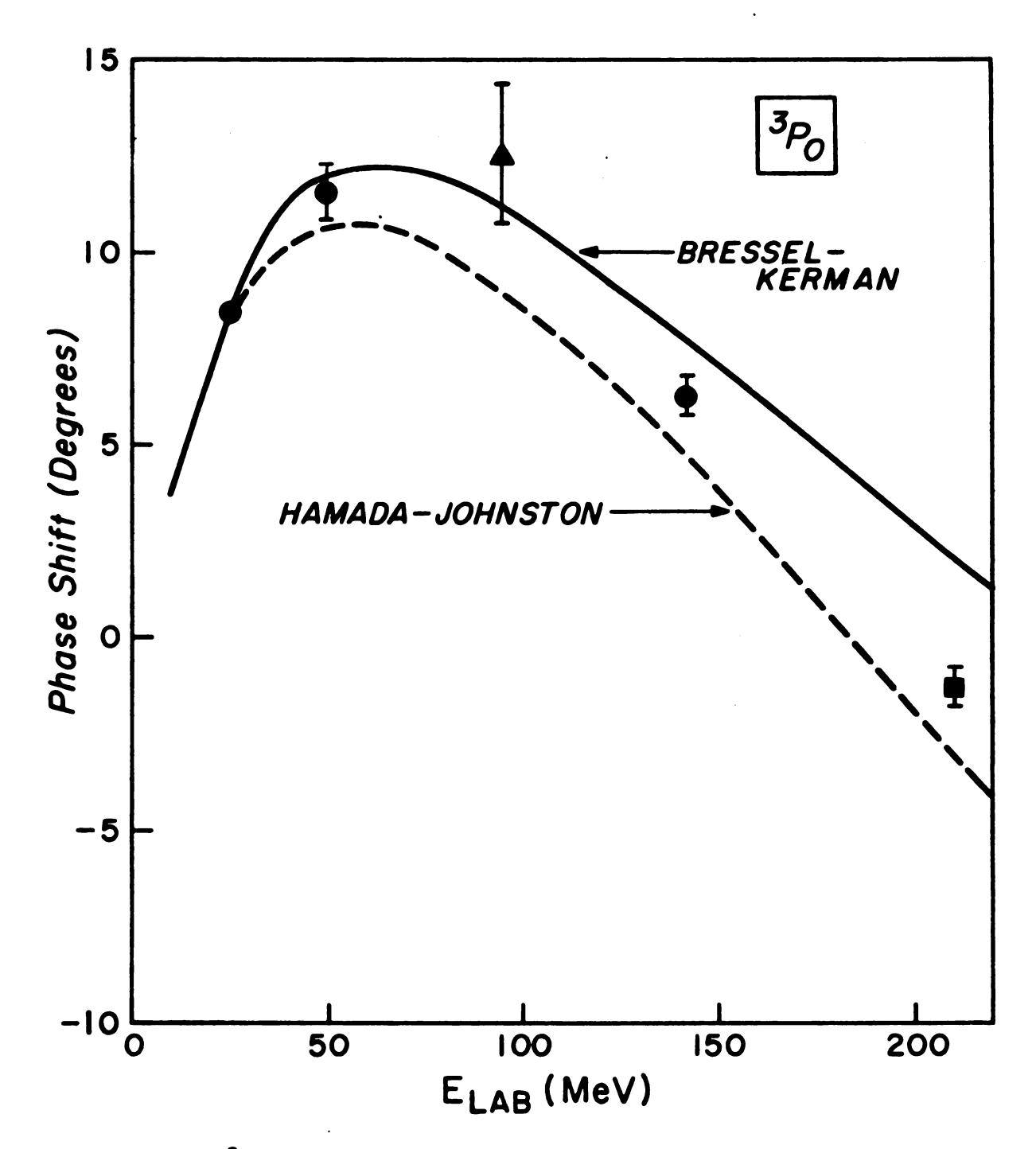


Figure 8. <sup>3</sup>P<sub>0</sub> phase shift vs. energy. Circles are from Reference 22, squares from Reference 4, and triangles from Reference 21.

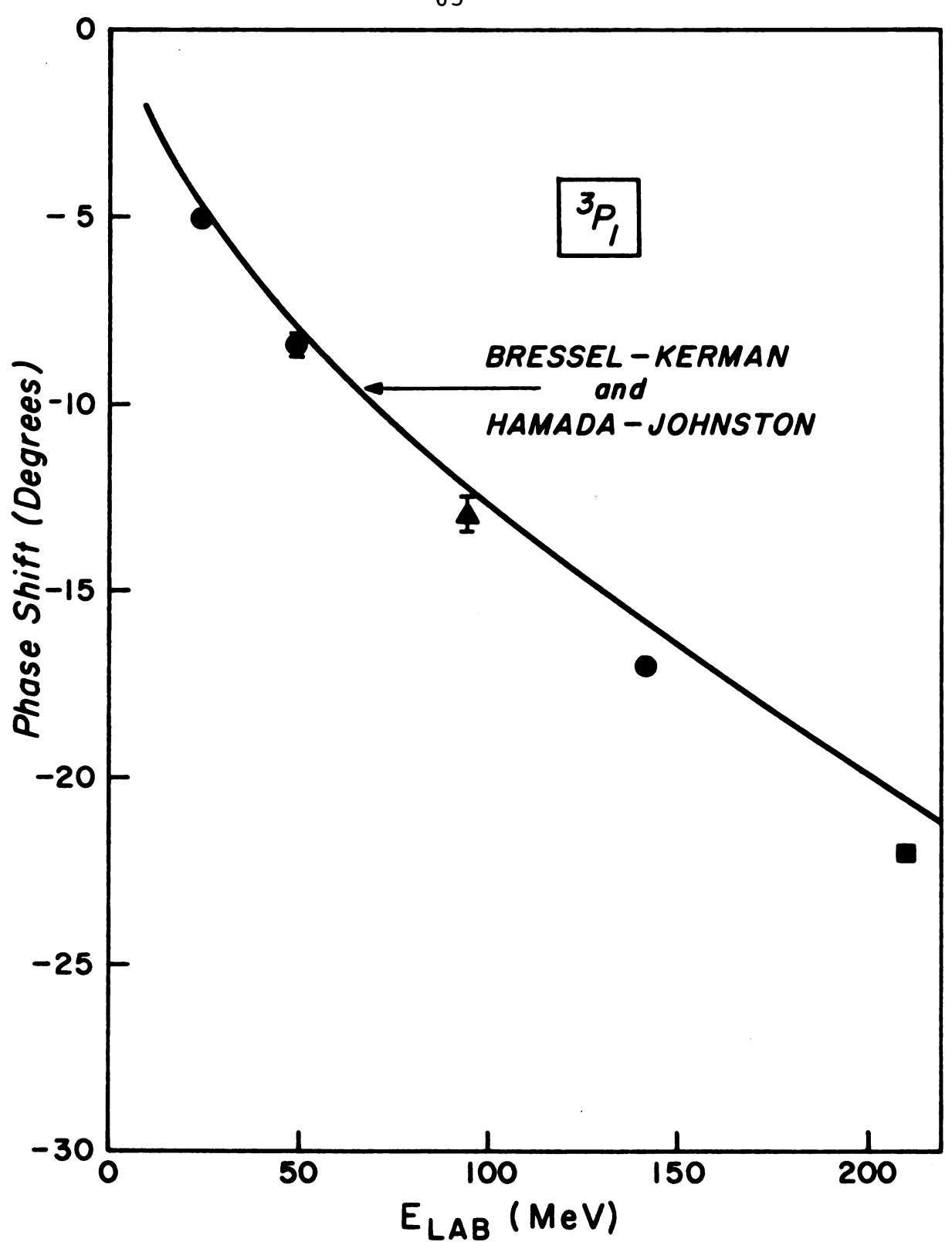


Figure 9. <sup>3</sup>P<sub>1</sub> phase shift vs. energy. Circles are from Reference 22, Squares from Reference 4, and triangles from Reference 21.

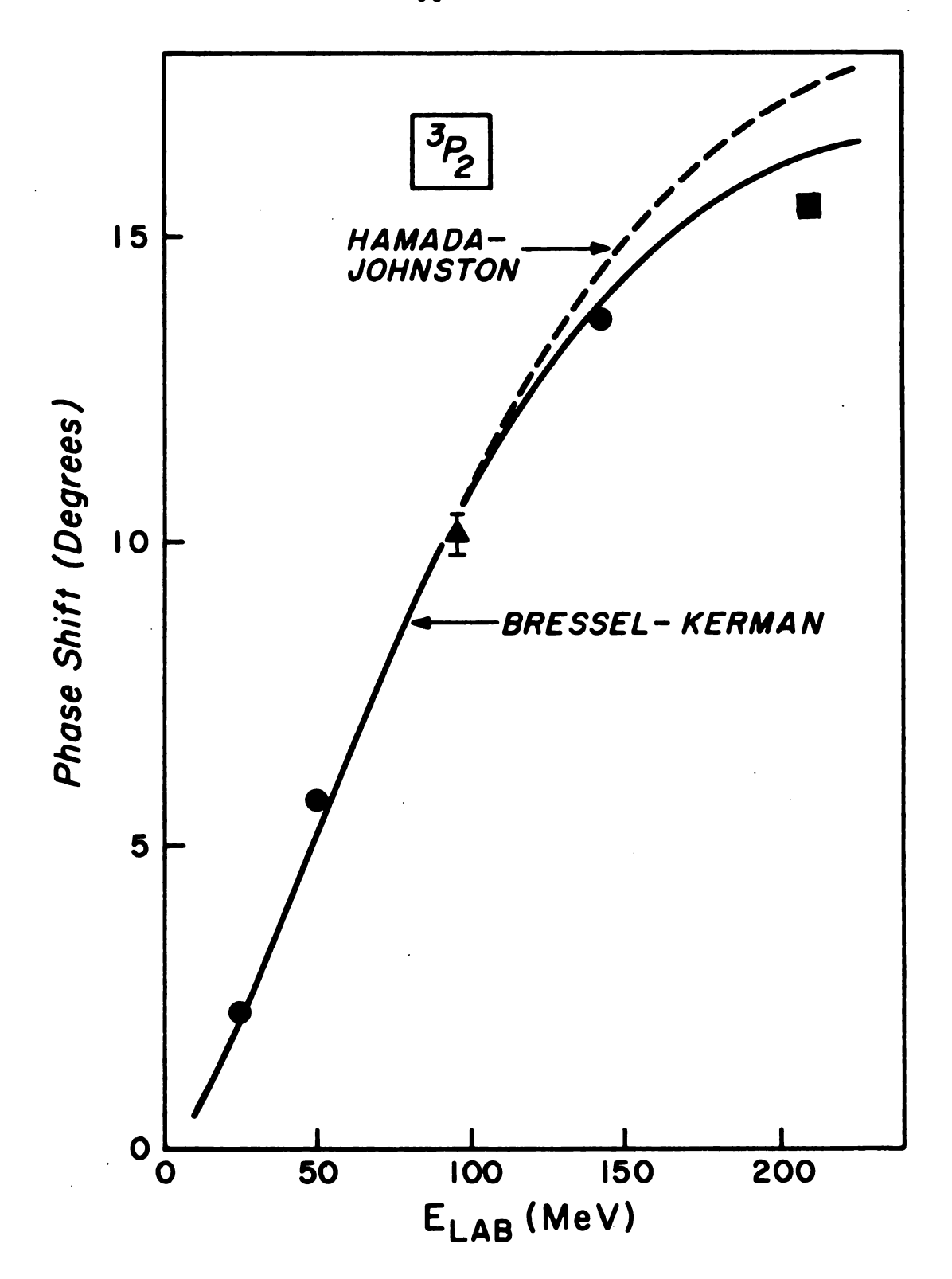
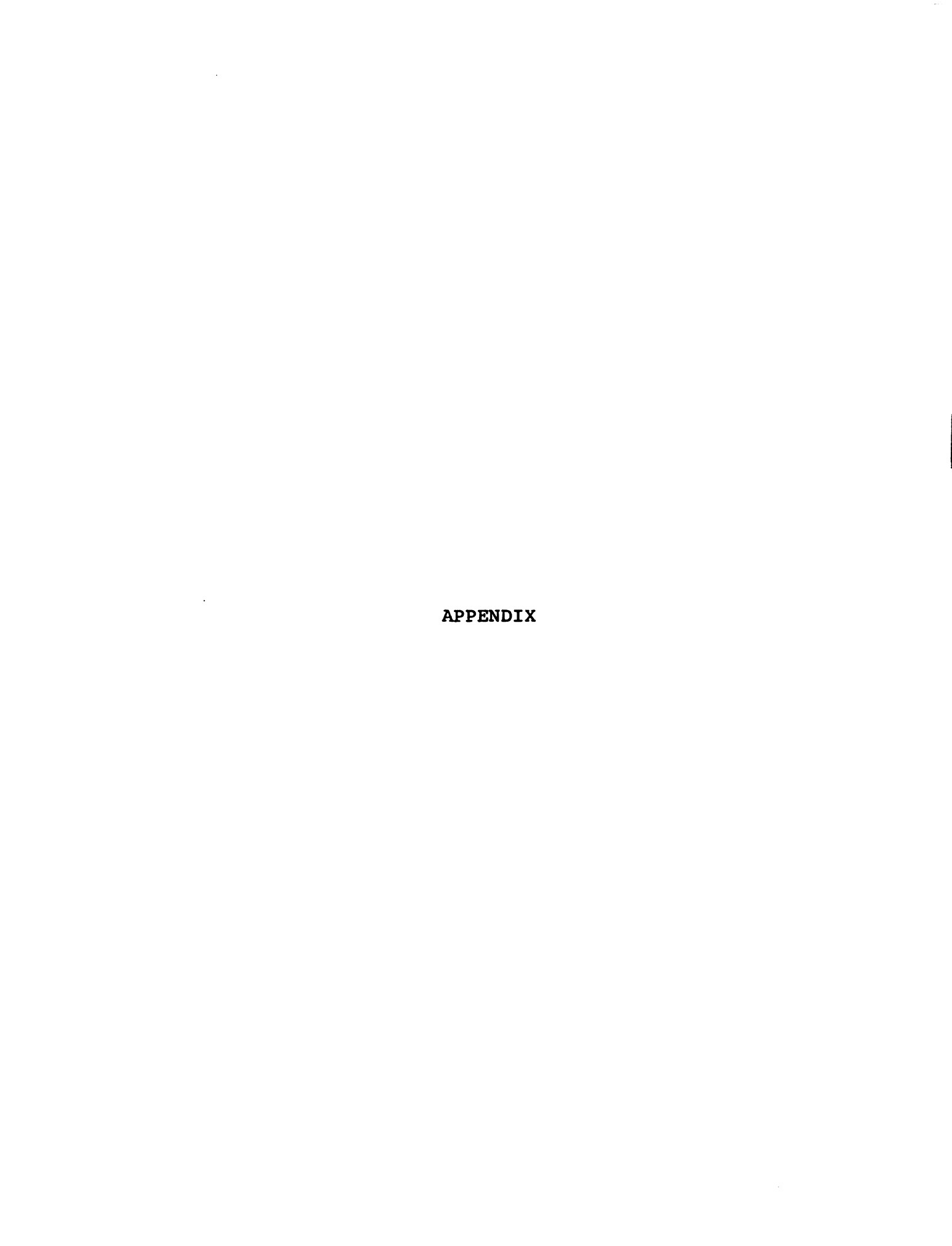


Figure 10. <sup>3</sup>P<sub>2</sub> phase shift vs. energy. Circles are from Reference 22, Squares from Reference 4, and triangles from Reference 21.

energy per particle which was in good agreement with the empirical value of 16 MeV. It would be desirable to repeat the work on the  $^3\mathrm{S}_1$ , P, and D states with a set of potentials similar to the ones used for the  $^1\mathrm{S}_0$  state rather than the Hamada-Johnston potential which is not always in agreement with the phase shifts obtained from analyses of the two-nucleon elastic scattering data.



## **APPENDIX**

## **DIAGRAMS**

The unperturbed ground state of nuclear matter is represented by a Slater determinant of the unperturbed single particle wave functions corresponding to the A single particle states of lowest energy. That is

$$\vec{p} = (A!)^{-\frac{1}{2}} \mathcal{Q} \prod_{i=1}^{A} \phi_i(\vec{r}_i)$$

where  $\mathcal Q$  is the antisymmetrizing operator. The unperturbed wave function,  $\mathcal Q_o$  , is normalized

Let  $\phi(\vec{r})$  and  $\phi(\vec{r})$  be two single particle states interacting through the two-nucleon potential. Then the product of these states is written

The matrix element describing the scattering of particles 1 and 2 through the two nucleon potential from states  $\rho$  and  $\varrho$  to states r and s is

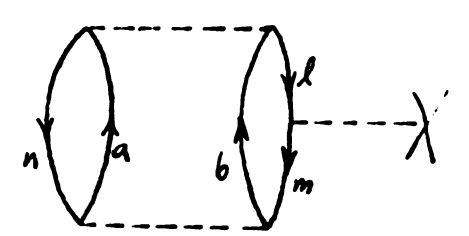
The matrix element of the single particle potential is similarly defined

Define the Fermion creation and annihilation operators with the properties that  $a_{\rho}^{\dagger}$  creates a particle (annihilates a hole) in state  $\rho$ , and  $a_{\rho}$  annihilates a particle (creates a hole) in state  $\rho$ . These operators satisfy the anticommutation relations

Diagrams provide a convenient way of illustrating the effect of a particular term in the Brueckner-Goldstone expansion. In order that they be used in a consistent way, it is necessary to specify a few rules for drawing or interpreting a diagram. The direction of increasing time will be toward the top of the page. Any state not specifically included in a diagram is assumed to be as it was in the unperturbed state. Thus above and below the diagram all states below the Fermi level are filled and all states above are empty. The first interaction results in two particles in the Fermi sea being excited to states above the Fermi sea, leaving holes in the originally occupied states. Continuing in the direction of increasing time, particles are repeatedly scattered into unoccupied states until the final interaction results in their being scattered back into their original states, leaving the wave function as it was before the first interaction took place. An upward directed line represents

a particle above the Fermi sea and a downward directed line represents a hole in the Fermi sea. Since particle number is conserved, there must always be one hole in the Fermi sea for every particle above it. The matrix element  $\langle \rho q/\nu/rs \rangle$ is represented by a horizontal dashed line connecting the intersection of lines representing the states  $\rho$  and r at one end with the intersection of lines representing states q and s at the other end. The matrix element  $\langle \rho/V/q \rangle$  is represented by a horizontal dashed line terminated at one end by the intersection of the lines representing states p and  $\varphi$  and at the other end by an  $\chi$  . The incoming lines are associated with the initial state  $/r_s>$  . The particles in this state are destroyed by the operator 9, 9, . The operator a creates particles in the final state which is represented by the outgoing lines. The energy denominator is equal to the sum of the particle energies minus the sum of the hole energies. Finally, the contribution of the diagram to the energy shift is obtained by multiplying the product of the matrix elements and the energy denominators by (-1) h+c+e+s where h is the number of hole lines, c is the number of closed loops, e is the number of energy denominators, and s is the number of interactions involving the single particle potential.

Consider, for example, the following diagram:



The initial state is just  $\mathcal{Q}_{\bullet}$ . As a result of the first two-body interaction, particles in states n and m in the Fermi sea are scattered into excited states a and b, respectively, leaving holes in the states they originally occupied. In operator notation this is written

$$a_a^{\dagger} a_b^{\dagger}$$
 an am  $|\bar{\Phi}_o\rangle$ 

The matrix element corresponding to this interaction is  $\langle ab/v/n_m \rangle$  and the energy denominator for the intermediate state resulting from this interaction is  $-(\bar{c_*} + \bar{c_*} - \bar{c_*} - \bar{c_*})^{-1}$ . The minus sign preceding this term will later be combined with other factors of -1 as described in the final rule in the previous paragraph. Thus the effect of the first interaction is written

$$-\frac{\langle ab/v/nm\rangle}{\langle \mathcal{E}_{n}+\mathcal{E}_{b}-\mathcal{E}_{m}-\mathcal{E}_{n}\rangle} a_{n}^{\dagger} a_{b}^{\dagger} a_{n} a_{m}$$

The interaction with the single particle potential results in the scattering of a particle in state  $\mathcal L$  in the Fermi sea into the unoccupied state m also in the Fermi sea, leaving a hole in state  $\mathcal L$ . It can also be thought of as the scattering of the hole in state m into state  $\ell$ . This interaction contributes the additional factor

$$-\frac{\langle m/V/l\rangle}{(\varepsilon_n+\varepsilon_p-\varepsilon_n-\varepsilon_2)} a_1 a_m^{\dagger}$$

to the term resulting from the first interaction. Although this interaction involves scattering from state m to  $\mathcal L$ , the energies of states  $\alpha$ , b, and n also affect the

contribution of this interaction. This is an example of a process taking place off the energy shell. The final interaction scatters the particles in excited states  $\alpha$  and  $\beta$  back into the holes left in states n and  $\beta$  as the result of the previous interactions. After this interaction the particles are all back in their unperturbed ground states. The total contribution of this diagram is

$$\frac{\langle nl | v | a b \rangle \langle m | v | l \rangle \langle ab | v | nm \rangle}{(E_a + E_b - E_n - E_e)(E_a + E_b - E_m - E_n)}$$

The quantity

is just **±1**, depending on the order of the creation and destruction operators. Using the commutation relations for the operators and remembering that

$$a_{p}^{\dagger}a_{p}/\bar{I}_{\bullet}\rangle =\begin{cases} /\bar{I}_{\bullet}\rangle & \text{if } p \leq A \text{ (in the Fermi sea)} \\ 0 & \text{if } p > A \text{ (above the Fermi sea)} \end{cases}$$

the expectation value of this particular set of operators is found to be +1. This agrees with the result obtained by using the last rule for the diagrams. There are three hole lines, two closed loops, and one interaction involving the single particle potential, giving a sign of (-1) 3+2+1=+1. The two minus signs from the energy denominators cancel, leaving as the contribution of this diagram to the energy of nuclear matter

$$\langle n l | v | a b \rangle \langle m | V | l \rangle \langle a b | v | n m \rangle$$
  
 $(\bar{\epsilon}_a + \bar{\epsilon}_b - \bar{\epsilon}_a - \bar{\epsilon}_a) (\bar{\epsilon}_a + \bar{\epsilon}_b - \bar{\epsilon}_m - \bar{\epsilon}_b)$ 

To find the total contribution of all the distinct diagrams of this type, one must calculate the sum of these terms where a and b are allowed to take on all possible values greater than A, and m, n, and l take on all possible values between 1 and A. The sum is then multiplied by  $\frac{1}{2}$  to account for the fact that since

each distinct combination of states has been calculated twice.

REFERENCES

## REFERENCES

- 1. P. Cziffra and M. J. Moravcsik, University of California Radiation Laboratory Report UCRL-8523 Rev.
- 2. C. B. Bressel and A. K. Kerman quoted in P. C. Bhargava and D. W. L. Sprung, Annals of Physics (N. Y.), 42, 222 (1967).
- 3. T. Hamada and I. D. Johnston, Nucl. Phys. 34, 382 (1962).
- M. D. Miller, P. S. Signell, and N. R. Yoder, Phys. Rev. 176, 1724 (1968).
- 5. M. S. Sher, Ph. D. thesis, Michigan State University, 1969.
- 6. G. A. Baker, Jr., Phys. Rev. 128, 1485 (1962).
- 7. R. E. Peierls, <u>Proceedings of the International</u>
  <u>Conference on Nuclear Structure, Kingston</u>, <u>University</u>
  of Toronto Press, Toronto, 1960.
- 8. A. M. Green, Nucl. Phys. <u>33</u>, 218 (1962) and A. M. Green, Phys. Lett. 1, 136 (1962).
- 9. K. A. Brueckner and K. S. Masterson, Jr., Phys. Rev. 128, 2267 (1962) hereafter referred to as BM.
- 10. J. Orear, A. H. Rosenfeld, and R. A. Schluter, Nuclear Physics, University of Chicago Press, Chicago, 1967, p. 7.
- 11. P. A. Seeger, Nucl. Phys. 25, 1 (1961).
- 12. A. E. S. Green, Phys. Rev. 95, 1006 (1964).
- 13. D. Halliday, <u>Introductory Nuclear Physics</u>, John Wiley & Sons, Inc., New York, 1962, p. 261.
- 14. B. H. Brandow, Ph. D. thesis, Cornell University, 1964 quoted in Reference 16.
- 15. Much of the material for this section was obtained from Reference 16.

- 16. B. Day, Rev. Mod. Phys. 39, 719 (1967).
- 17. M. W. Kirson, Nucl. Phys. A99, 353 (1967).
- 18. S. Okubo and R. E. Marshak, Annals of Physics 4, 166 (1958) quoted in P. Signell, The Nuclear Potential, in Advances in Nuclear Physics, M. Baranger and E. Vogt, ed., Vol. 2, Plenum Press, New York, 1969.
- 19. L. Ingber, Ph. D. thesis, University of California, San Diego, 1967.
- 20. K. A. Brueckner and J. L. Gammel, Phys. Rev. <u>109</u>, 1023 (1958).
- 21. P. S. Signell and M. D. Miller, Phys. Rev. <u>178</u>, 2377 (1969).
- 22. M. H. MacGregor, R. A. Arndt, and R. M. Wright,
  University of California preprint UCRL 70075 (Part X).

